Malignant Perinatal Variant of Long-QT Syndrome Caused by a Profoundly Dysfunctional Cardiac Sodium Channel

Dao W. Wang, MD, PhD; Lia Crotti, MD, PhD; Wataru Shimizu, MD, PhD; Matteo Pedrazzini, BSc; Francesco Cantu, MD; Paolo De Filippo, MD; Kanako Kishiki, MD; Aya Miyazaki, MD; Tomoaki Ikeda, MD, PhD; Peter J. Schwartz, MD; Alfred L. George Jr, MD

Background—Inherited cardiac arrhythmia susceptibility contributes to sudden death during infancy and may contribute to perinatal and neonatal mortality, but the molecular basis of this risk and the relationship to genetic disorders presenting later in life is unclear. We studied the functional and pharmacological properties of a novel de novo cardiac sodium channel gene (*SCN5A*) mutation associated with an extremely severe perinatal presentation of long-QT syndrome in unrelated probands of different ethnicity.

Methods and Results—Two subjects exhibiting severe fetal and perinatal ventricular arrhythmias were screened for *SCN5A* mutations, and the functional properties of a novel missense mutation (G1631D) were determined by whole-cell patch clamp recording. In vitro electrophysiological studies revealed a profound defect in sodium channel function characterized by ≈10-fold slowing of inactivation, increased persistent current, slowing of recovery from inactivation, and depolarized voltage dependence of activation and inactivation. Single-channel recordings demonstrated increased frequency of late openings, prolonged mean open time, and increased latency to first opening for the mutant. Subjects carrying this mutation responded clinically to the combination of mexiletine with propranolol and survived. Pharmacologically, the mutant exhibited 2-fold greater tonic and use-dependent mexiletine block than wild-type channels. The mutant also exhibited enhanced tonic (2.4-fold) and use-dependent block (≈5-fold) by propranolol, and we observed additive effects of the 2 drugs on the mutant.

Conclusions—Our study demonstrates the molecular basis for a malignant perinatal presentation of long-QT syndrome, illustrates novel functional and pharmacological properties of *SCN5A*-G1631D, which caused the disorder, and reveals therapeutic benefits of propranolol block of mutant sodium channels in this setting. **(*Circ Arrhythmia Electrophysiol.* 2008;1:370-378.)**

Key Words: antiarrhythmia agents ■ arrhythmia ■ death, sudden ■ heart arrest ■ ion channels

Sudden unexplained death attributable to cardiac arrhythmia may occur at any age. When death occurs during infancy for no apparent reason, a diagnosis of the sudden infant death syndrome (SIDS) may be appropriate.[1,2] Recent evidence suggests that 9% to 10% of SIDS victims carry germ line mutations in arrhythmia susceptibility genes such as those associated with the congenital long-QT syndrome (LQTS).[3] Anecdotally, ventricular arrhythmias occurring during the perinatal or neonatal periods are associated with a poor prognosis and a low survival rate.[4–7] Whether cardiac arrhythmia susceptibility presenting in early life represents a biologically distinct disease is an unanswered question.

Clinical Perspective see p 378

Mutations in *SCN5A* encoding the cardiac voltage-gated sodium channel $Na_v1.5$ have been associated with a spectrum of increased sudden death risk extending from fetal life to adulthood. Recurrent third trimester fetal loss has been observed in the setting of occult *SCN5A* mutations.[8] In older children and adults with LQTS of known genotype, only ≈10% carry mutations in *SCN5A*,[9–11] but the proportion of *SCN5A* mutations among SIDS victims with an LQTS gene defect approaches 50%.[3] Further, among older children and adults with LQTS those individuals harboring *SCN5A* mutations exhibit a greater likelihood of severe symptoms including sudden death when compared with the majority of

Received April 24, 2008; accepted September 15, 2008.

From the Department of Medicine (D.W.W., A.L.G.), Vanderbilt University, Nashville, Tenn; Section of Cardiology (L.C., P.J.S.), Department of Lung, Blood and Heart, University of Pavia; Department of Cardiology (L.C., P.J.S.) and Molecular Cardiology Laboratory (L.C., M.P., P.J.S.), IRCCS Fondazione Policlinico S. Matteo, Pavia, Italy; Division of Cardiology (W.S.), Department of Internal Medicine, Department of Pediatric Cardiology (K.K., A.M.), Department of Perinatology (T.I.), National Cardiovascular Center, Osaka, Japan; Department of Cardiology (F.C., P.D.F.), Ospedali Riuniti, Bergamo, Italy; Department of Pharmacology (A.L.G.), Vanderbilt University, Nashville, Tenn.

The online-only Data Supplement is available at http://circep.ahajournals.org/cgi/content/full/1/5/378/DC1.

Correspondence to Alfred L. George Jr, MD, Division of Genetic Medicine, 529 Light Hall, Vanderbilt University, Nashville TN 37232-0275. E-mail al.george@vanderbilt.edu

Circ Arrhythmia Electrophysiol **is available at http://circep.ahajournals.org** **DOI: 10.1161/CIRCEP.108.788349**

individuals who carry mutations in 2 potassium channel genes (*KCNQ1*, *KCNH2*).[9,11] The higher proportion of *SCN5A* mutations among SIDS victims with known genotype when compared with older LQTS subjects might be explained by negative selection for more deleterious alleles. Support for this hypothesis requires evidence that mutations with greater functional consequences are responsible for severe and earlier onset arrhythmia syndromes.

Here, we present an extensive characterization of a novel *SCN5A* mutation that occurred de novo in unrelated and ethnically distinct newborns. In mutation carriers, life-threatening ventricular arrhythmias occurred within hours of birth. The mutation caused a profound degree of sodium channel dysfunction that was more severe than that observed for any previous *SCN5A* variant. Despite the extreme nature of the mutation and the associated dire clinical scenario, the subjects survived owing to prompt therapeutic interventions including treatment with the combination of mexiletine and propranolol, 2 drugs that exhibited enhanced and additive activity against the mutant allele. These observations illustrate the role of severe sodium channel mutations in a malignant perinatal variant of LQTS and successful use of combination pharmacotherapy to prevent perinatal mortality in this setting.

Methods

Molecular Genetics

Informed consent for performing genetic studies was obtained using methods approved by the Ethics Review Board of IRCCS Fondazione Policlinico San Matteo (Pavia, Italy) or by the Institutional Research Board and Ethics Committee and the Committee on Genetic Analysis and Gene Therapy of the National Cardiovascular Center (Suita, Japan). Genomic DNA was isolated from whole blood and coding exons of *SCN5A*, *KCNQ1*, *KCNH2*, *KCNE1*, and *KCNE2* were screened for genetic variants using previously described methods.[12,13]

Mutagenesis and Heterologous Expression of Na Channels

Mutations were engineered in a human heart sodium channel ($Na_V1.5$) cDNA (hH1) using recombinant polymerase chain reaction. Final constructs were assembled in the mammalian expression plasmid pRc/CMV-hH1 and then sequenced to verify creation of the mutation and to exclude polymerase errors. Cells (tsA201) were transiently transfected with pRc/CMV-hH1 or mutants using FuGene6 (Roche Diagnostics) combined with a bicistronic plasmid (pEGFP-IRES-hβ1) encoding enhanced green fluorescent protein and the human β1 subunit (hβ1) under the control of the cytomegalovirus immediate early promoter. Additional methods are provided in an online supplement.

Statement of Responsibility

The authors had full access to the data and take responsibility for its integrity. All authors have read and agree to the manuscript as written.

Results

Malignant Perinatal Arrhythmia Associated With a Novel *SCN5A* Mutation

We identified a novel *SCN5A* mutation in 2 unrelated newborns that experienced life-threatening perinatal ventricular arrhythmias. The first subject was an Italian male

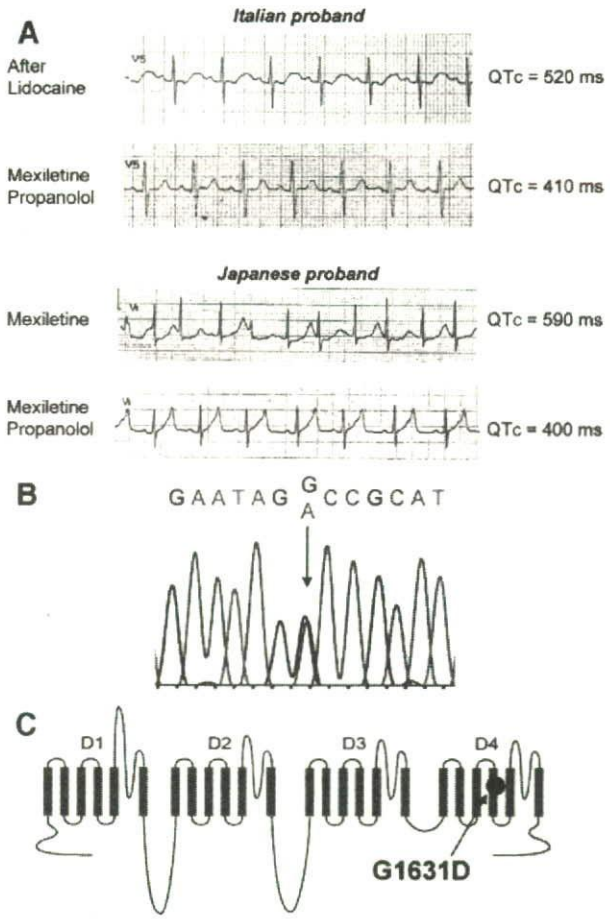

Figure 1. Electrocardiographic responses to pharmacotherapy and genotype of probands. A, Representative ECG traces (lead V5) showing responses to mexiletine and propranolol for the Italian and Japanese probands. Rate-corrected QT interval (QTc) measurements are indicated to the right of each tracing. B, Sequencing electropherogram (Italian proband) illustrating heterozygosity for a G to A mutation corresponding to G1631D. C, Location of G1631D in the predicted transmembrane topology of $Na_V1.5$.

delivered by emergency C-section at 32-weeks gestation for abnormal fetal heart rhythm. Initially, he appeared healthy (APGAR score 8) but then, within hours of his birth, developed polymorphic ventricular tachycardia with periods of bradycardia and frequent premature ventricular beats. Initial treatments with intravenous magnesium and isoproterenol were not effective, but administration of intravenous lidocaine suppressed ventricular arrhythmias and restored sinus rhythm revealing a prolonged QTc interval (520 ms). Empirical treatment with propranolol (1.3 mg/kg/d) and mexiletine (11 mg/kg/d) controlled arrhythmias and normalized the QTc (410 ms) (Figure 1A). One month after discharge, the infant survived an episode of ventricular fibrillation. Ventricular arrhythmia was further controlled by rapid pacing (120 bpm) with increased dosages of propranolol (3 mg/kg/d) and mexiletine (16 mg/kg/d). During the following 12 months, the child exhibited no further ventricular arrhythmias but required recurrent hospitalizations for paroxysmal atrial flutter that was eventually controlled by

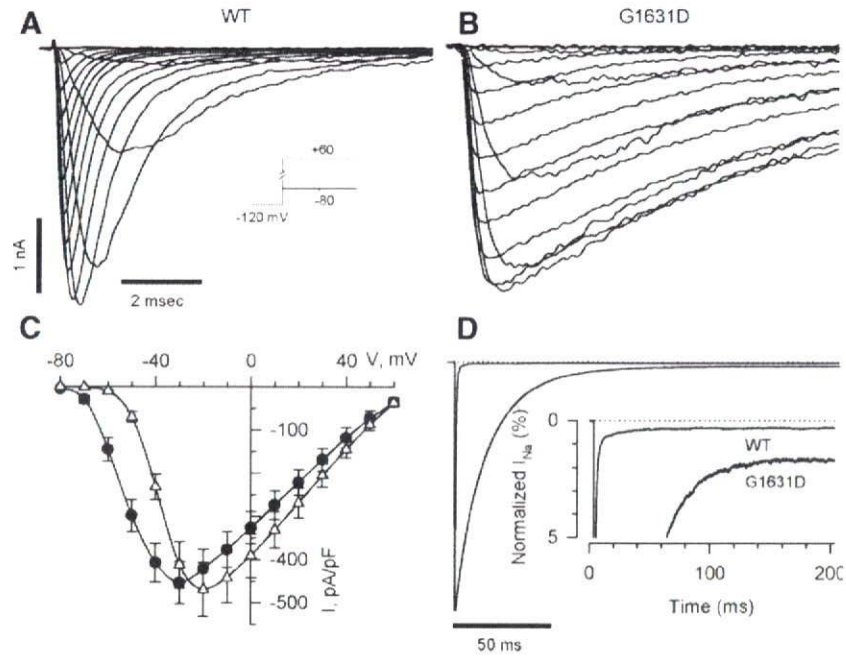

Figure 2. Whole-cell current recordings of WT and G1631D sodium channels. Representative sodium currents recorded from cells expressing WT (A) or G1631D (B) elicited by depolarizing steps from −80 mV to +60 mV in 10-mV increments from holding potential −120 mV. C, Comparison of current-voltage relationships for WT (n=15) and G1631D (n=16). Current is normalized to cell capacitance to give sodium current density. D, Increased tretrodotoxin (TTX)-sensitive persistent sodium currents for G1631D. Peak sodium currents were normalized. The zero-current level is indicated by a dotted line. The inset shows an expanded *y* axis scaled to emphasize the relative proportion of persistent current for WT (n=8) and G1631D (n=9).

ablation. The child has survived beyond the age of 26 months without further ventricular or atrial arrhythmias.

The second proband was a Japanese male delivered by emergency C-section at 34-weeks gestation because of ventricular arrhythmia (torsade de pointes, TdP) documented in utero by magnetocardiography. Initial APGAR scores were 8 and 9, but his QTc interval was 567 ms and he had multiple episodes of TdP. Intravenous injection (3 mg/kg) followed by continuous infusion of mexiletine abolished TdP. He was discharged on oral mexiletine (20 mg/kg/d) but was readmitted for treatment of recurrent TdP approximately 2 months later (QTc=590 ms). Continuous infusion of mexiletine combined with oral mexiletine (serum drug concentration: 1.3 to 1.4 μg/mL) considerably abbreviated the QTc (462 to 499 ms) but did not completely suppress episodes of TdP. The addition of continuous infusion propranolol (0.5 mg/kg/d, serum drug concentration: 18.4 to 25.1 ng/mL) further shortened QTc (395 to 424 ms) and fully suppressed ventricular arrhythmias. Finally, combination therapy with oral mexiletine and oral propranolol was effective in suppressing ventricular arrhythmias through age 8 months (Figure 1A).

A novel *SCN5A* missense mutation (G1631D) was discovered in both probands (Figure 1B). Family histories were negative for arrhythmia syndromes. The results of ECG testing were normal for both sets of parents, and they were mutation negative. Paternity testing demonstrated that the mutation was de novo in both cases. No other mutations were identified in *SCN5A*, *KCNQ1*, *KCNH2*, *KCNE1*, or *KCNE2* in either proband.

Profound Dysfunction of G1631D Channels

The mutation results in substitution of a highly conserved glycine residue with a negatively charged glutamic acid in the S4 segment of domain 4 (D4/S4; Figure 1C). This residue is 100% conserved in all known voltage-gated sodium channel sequences from several diverse phyla. This structural domain in sodium channels participates as a component of the voltage-sensor important for activation and inactivation.[14,15] Introduction of a negatively charged side group into this domain was predicted to have a significant functional effect. To test this hypothesis, we engineered G1631D in recombinant human $Na_V1.5$ for heterologous expression and then performed electrophysiological studies.

Figure 2 illustrates the general functional properties of wild-type (WT) and mutant $Na_V1.5$ channels expressed heterologously in human tsA201 cells. Representative whole-cell current tracings demonstrate that the mutant exhibits a profound level of dysfunction characterized by substantial delays in activation and inactivation. Overall current density was similar between cells expressing WT or mutant channels but there was a positive shift in the peak current-voltage (I-V) relationship for the mutant (Figure 2C). Mutant channels exhibited increased steady-state persistent current measured 200 ms after the peak transient current (Figure 2D; persistent current as % of peak current: WT, 0.31±0.04%, n=8; G1631D, 1.63±0.31%, n=9; $P<0.001$). Although increased persistent current is characteristic of *SCN5A* mutations associated with LQTS,[16,17] no previously characterized mutation had such a profound inactivation defect.

Figure 3 illustrates quantitative assessments of activation and inactivation. Mutant channels exhibited a global slowing of activation across the range of tested potentials as assessed by time to peak current (Figure 3A). Similarly, G1631D exhibited a profound slowing of inactivation as illustrated by the voltage dependence of inactivation time constants (Figure 3B). The degree of slowing of inactivation was approximately 10-fold compared with WT. The mutant also exhibited significant depolarizing shifts in the voltage dependence of activation (+12 mV) and steady-state inactivation (+14 mV; Figure 3C and 3D; supplemental Table I, available online). These asymmetrical depolarizing shifts in activation and steady-state inactivation predict an increased window current

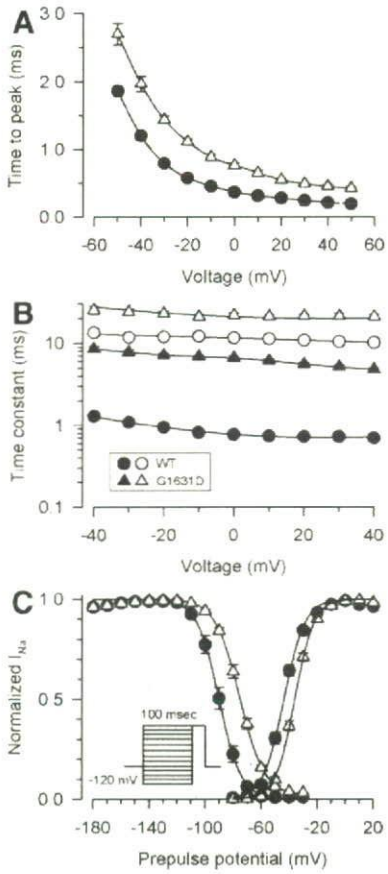

Figure 3. Activation and inactivation of WT and mutant channels. A, Time to peak activation in the voltage range of −50 to +50 mV. Differences between WT (n=15) and G1631D (n=16) were significant at the $P<0.001$ level for all tested voltages. B, Voltage dependence of inactivation time constants (same number of replicates as in A). Filled and open symbols indicate fast and slow component values, respectively. C, Voltage dependence of activation and steady-state inactivation elicited by a 100-ms conditioning pulse to various voltages (same number of replicates as in A).

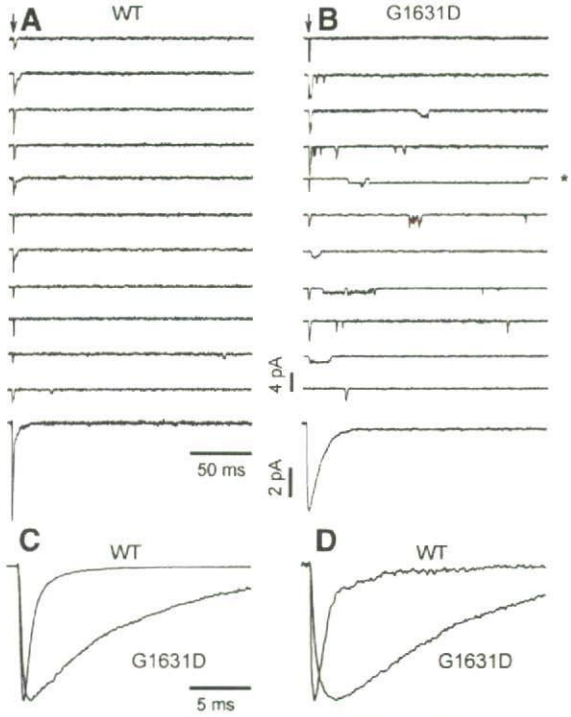

Figure 5. Single-channel properties of WT and G1631D channels. Sodium channel activities recorded at −20 mV from a multichannel outside-out patch excised from a cell expressing WT (A) or G1631D (B). Vertical arrows indicate the onset of patch depolarization from −120 mV to −20 mV. Lower traces show the ensemble averaged current obtained from 100 consecutive traces for WT and G1631D, respectively. C and D are comparisons of normalized and superimposed current traces of WT and G1631D at test potential of −20 mV from whole-cell recordings (C) and single-channel recordings (D).

defined as the overlap of these 2 curves (see Supplemental Figure I).

In Figure 4A, the time course of recovery from inactivation after a 100-ms conditioning pulse illustrates that the mutant has profound slowing of recovery. This difference was explained by a larger slow component of recovery from inactivation as determined by double exponential fitting (see Supplemental Table I). For WT channels, the majority of recovery occurs with a time constant of approximately 10 ms. By contrast for G1631D channels, the predominant fraction of channels recover from inactivation with a time constant of approximately 100 ms. The marked slowing of recovery from inactivation exhibited by G1631D correlated with a greater loss of channel availability during repetitive membrane depolarizations at frequencies exceeding 1 Hz (Figure 4B).

These profound gating abnormalities were correlated with aberrant single-channel events. Figure 5 illustrates representative single-channel recordings from cells expressing WT or mutant channels. Wild-type channels exhibited brief and transient openings clustered at the onset of the test depolarization. By contrast, the mutant exhibited a marked increase

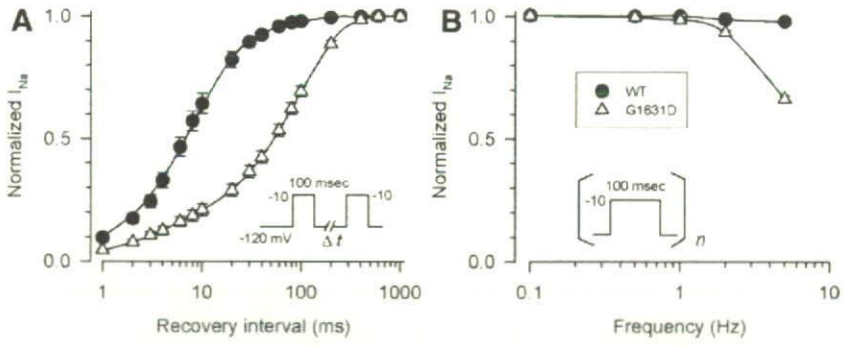

Figure 4. Recovery from inactivation. A, Time course of recovery from inactivation for WT (n=12) and G1631D (n=16) was elicited using the 2-pulse protocol shown in the inset. Time constants and fractional amplitudes are given in supplemental Table I. B, Activity dependent loss of channel availability following trains of 100 ms pulses to −10 mV from a holding potential of −120 mV applied at the frequency indicated (n=10 to 18 cells). Residual current following the 100th pulse was normalized to the first pulse current amplitude.

in probability of late reopenings and occasional prolonged openings (asterisk). Single-channel conductance levels were similar for WT (24pS) and G1631D (25pS), but mutant channels exhibited significantly longer latency to first opening (WT: 0.59±0.03 ms; G1631D: 1.15±0.03 ms; n=3; $P<0.001$), increased mean open time (WT: 0.34±0.09 ms; G1631D: 0.98±0.03 ms; n=3; $P=0.029$), and increased NP_o (WT: 0.14±0.02; G1631D: 0.22±0.03; n=3; $P=0.042$) when assessed at a test pulse of −20 mV. Ensemble averaged currents derived from single-channel records closely resemble those obtained from whole-cell recordings. These findings collectively indicate that G1631D causes a fundamental defect in channel activation and inactivation associated with dramatic clinical consequences.

Enhanced Mexiletine Sensitivity of G1631D Channels

Despite the profound nature of the sodium channel dysfunction caused by G1631D, both probands survived likely because of prompt intervention including pharmacological treatments. We compared the effect of mexiletine on WT and mutant channels. Figure 6A illustrates the responses of WT and G1631D to repetitive membrane depolarizations delivered at a frequency of 1 Hz in the presence of mexiletine (100 μmol/L). Both channels exhibited an initial drop in channel availability followed by further use-dependent loss of activity, but the effect is substantially greater for G1631D suggesting that the mutant has enhanced mexiletine sensitivity. Concentration-response relationships for tonic (Figure 6B) and use-dependent (Figure 6C) mexiletine block of WT and G1631D supported this hypothesis. Mexiletine block of WT channels exhibited EC_{50} values of 120.9 μmol/L and 50.9 μmol/L for tonic and use-dependent block, respectively. By contrast, G1631D was 1.8-fold and 2.8-fold more sensitive to tonic (EC_{50} 66.7 μmol/L) and use-dependent (EC_{50} 18.3 μmol/L) mexiletine block, respectively. Further, mexiletine induced a hyperpolarizing shift in steady-state inactivation of mutant channels such that this property became more similar to WT channels (G1631D $V_{½}$: no drug, −74.8±1.1 mV, n=16; 3 μmol/L mexiletine, −85.5±1.3 mV, n=9; $P<0.001$). By contrast, the same drug concentration has no significant effect on steady-state inactivation of WT channels (WT $V_{½}$: no drug, −89.3±1.1 mV, n=16; 3 μmol/L mexiletine, −86.6±3.2 mV, n=6; NS). Mexiletine also had moderate effects on the kinetics of G1631D inactivation (Figure 6B and 6C), illustrated by significant reductions in the time constants for inactivation, and significantly reduced the level of persistent current (no drug: 1.63±0.31%, n=9; 10 μmol/L mexiletine, 0.54±0.06%, n=8; $P=0.0098$).

Propranolol Block of WT and G1631D Channels

We also considered the role of propranolol in modulating mutant sodium channel behavior. Propranolol is a widely used β-adrenergic receptor antagonist, but early studies indicated that this drug also exhibits antiarrhythmic (membrane stabilizing) properties at high serum concentrations possibly from effects on voltage-gated sodium channels.[18,19] Figure 7A illustrates that both WT and G1631D channels are blocked by 3 μmol/L propranolol during repetitive stimula-

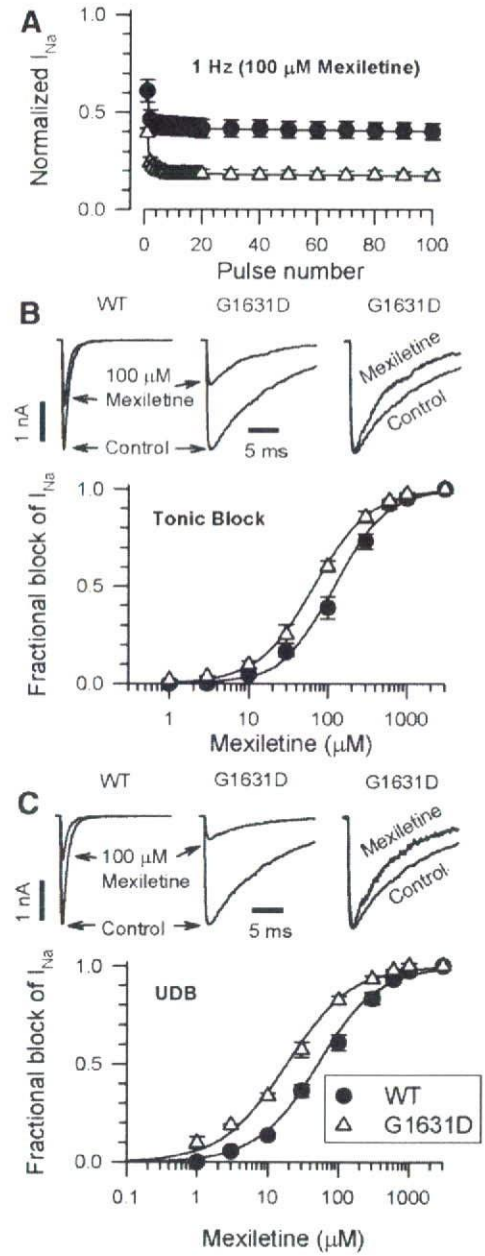

Figure 6. Effects of mexiletine on WT and G1631D. A, Mexiletine (100 μmol/L) block of WT (n=8) and G1631D (n=8) during a 1-Hz train of depolarizing pulses to −10 mV from a holding potential of −120 mV. B, Tonic mexiletine block of WT and G1631D. Upper traces (left, middle) illustrate the effects of 100 μmol/L mexiletine during a single depolarizing voltage step to −10 mV. Normalized traces (right) recorded in the absence (control) or presence of drug illustrate the effect of mexiletine on the inactivation time course. The plot illustrates the concentration-response relationships for tonic block by mexiletine (each data point represents the mean of 4 to 12 cells). C, Use-dependent mexiletine block of WT and G1631D. Upper traces (left, middle) illustrate the steady-state effects of 100 μmol/L mexiletine during a 1-Hz pulse train. Normalized traces (right) recorded in the absence (control) or presence of drug (100th pulse) illustrate the effect of mexiletine on the inactivation time course. Time constants in the absence of drug were: τ_1=7.7±0.7 ms, τ_2=19.7±0.6 ms, n=8; and in the presence of 100 μmol/L mexiletine: τ_1=4.5±0.7 ms, τ_2=10.9±1.0 ms, n=8 ($P=0.0095$ for τ_1; $P<0.0001$ for τ_2). The plot illustrates the concentration-response relationships for use-dependent block by mexiletine (each data point represents the mean of 4 to 12 cells). The lines in B and C were fit to the data according to the Hill equation.

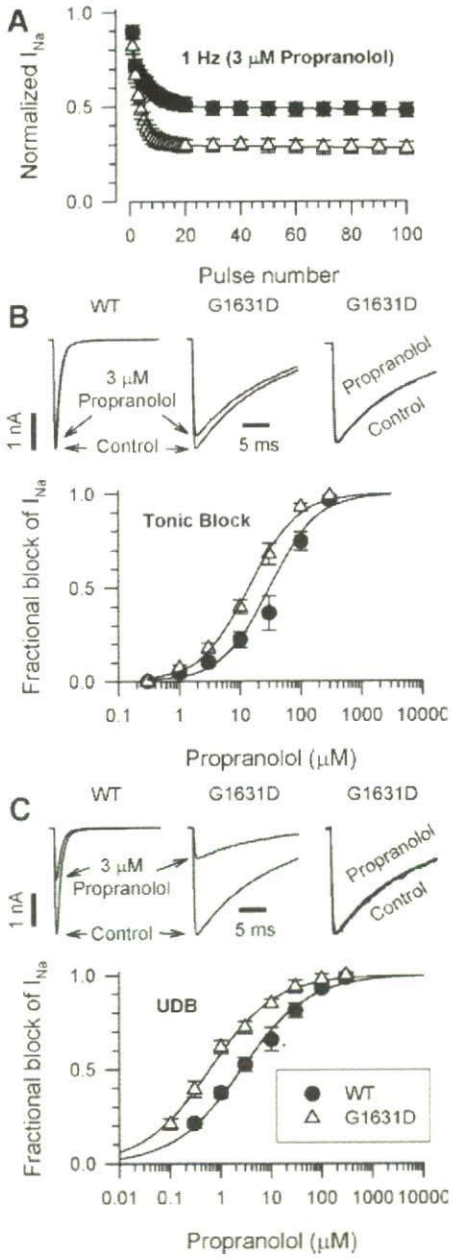

Figure 7. Effects of propranolol on WT and G1631D. A, Propranolol (3 μmol/L) block of WT (n=5) and G1631D (n=4) during a 1-Hz train of depolarizing pulses to −10 mV from a holding potential of −120 mV. B, Tonic propranolol block of WT and G1631D. Upper traces (left, middle) illustrate the effects of 3 μmol/L propranolol during a single depolarizing voltage step to −10 mV. Normalized traces (right) recorded in the absence (control) or presence of drug illustrate the effect of propranolol on the inactivation time course. The plot illustrates the concentration-response relationships for tonic block by propranolol (each data point represents the mean of 4 to 11 cells). C, Use-dependent propranolol block of WT and G1631D. Upper traces (left, middle) illustrate the steady-state effects of 3 μmol/L propranolol during a 1-Hz pulse train. Normalized traces (right) recorded in the absence (control) or presence of drug (100th pulse) illustrate the effect of propranolol on the inactivation time course. Time constants in the absence of drug were: τ_1=7.8±0.5 ms, τ_2=19.5±0.7 ms, n=4; and in the presence of 3 μmol/L propranolol: τ_1=6.9±1.1 ms, τ_2=18.1±1.0 ms n=4 (no significant differences in τ_1 or τ_2). The plot illustrates the concentration-response relationships for use-dependent block by propranolol (each data point represents the mean of 4 to 11 cells). The lines in B and C were fit to the data according to the Hill equation.

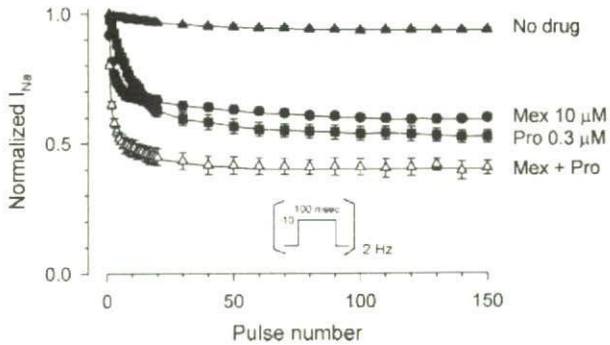

Figure 8. Effects of mexiletine with or without propranolol on G1631D channels. Sodium current was measured sequentially during a 2-Hz train of depolarizing pulses to −10 mV from a holding potential of −120 mV and values normalized to the current level after the initial pulse. Steady-state residual normalized sodium current after the 150th pulse was significantly lower for the combination of 10 μmol/L mexiletine with 0.3 μmol/L propranolol (fractional residual current, 0.4±0.03, n=3), when compared with either drug alone (mexiletine, 0.6±0.02; n=6; P=0.0039; propranolol, 0.5±0.03; n=6; P=0.041).

tion (1 Hz). Mutant channels exhibited a greater degree of steady-state block than WT channels under these conditions. Concentration-response curves demonstrated that propranolol exerts greater tonic (Figure 7B) and use-dependent (Figure 7C) block of G1631D than that of WT channels. Propranolol use-dependent block was enhanced 5-fold by the mutation (EC_{50}: WT, 3.0 μmol/L; G1631D, 0.6 μmol/L). The effect of propranolol, a racemic mixture, was not likely mediated through endogenous β-adrenergic receptors in the heterologous cell system because we observed similar blocking potency for R-(+)-propranolol, which has no receptor antagonist properties (see supplemental Figure II). Propranolol at a concentration similar to that observed in the Japanese proband (0.1 μmol/L) normalized steady-state inactivation of mutant channels (G1631D $V_{½}$: no drug, −74.8±1.1 mV, n=16; propranolol, −84.5±1.7 mV, n=10; P<0.001) but had no effect on steady-state inactivation of WT channels (WT $V_{½}$: no drug, −89.3±1.1 mV, n=16; propranolol, −88.8±0.9 mV, n=5; NS). Propranolol did not affect the kinetics of inactivation for WT or mutant channels (Figure 7B and 7C) or the level of persistent current observed for G1631D (no drug: 1.63±0.31, n=9; 1 μmol/L propranolol, 1.44±0.29, n=9; NS).

Because both probands responded clinically to the combination of mexiletine and propranolol, we tested the effects of both drugs together on G1631D channels. To closely simulate the clinical conditions, we tested use-dependent block at 2 Hz, which was the approximate resting heart rate of the Japanese proband and the frequency of cardiac pacing in the Italian child. The combination of mexiletine (10 μmol/L) and propranolol (0.3 μmol/L) caused a substantial loss of channel availability during a 2-Hz pulse train (Figure 8) when compared with the drug-free condition. The level of channel inhibition observed for the combination of mexiletine and propranolol was greater than either drug applied alone indicating additive effects.

Discussion

During late fetal development through shortly after birth, there is a vulnerable period when death occurs at a rate of 6 to 12 per 1000 live births per year,[20] and congenital arrhythmia susceptibility may be a significant contributor to this problem.[21,22] Life-threatening cardiac arrhythmias during infancy and the perinatal period may go unnoticed owing to the lack of routine use of electrocardiographic monitoring of the fetus and newborn. Studies of 2 large series of autopsied SIDS victims demonstrated that up to 10% of SIDS cases may represent genetic disorders of congenital arrhythmia susceptibility such as the LQTS,[3,23] short-QT syndrome,[24,25] and catecholaminergic polymorphic ventricular tachycardia.[26] Understanding the genetic risks for perinatal mortality should promote efforts to identify and treat at-risk newborns.

Malignant Perinatal Variant of LQTS

The profoundly dysfunctional *SCN5A* mutation, G1631D, produced a clinical entity distinct from typical LQTS (LQT3 subtype). Clinically, subjects with typical LQTS first develop symptoms (syncope, cardiac arrest, and sudden death) during late childhood, adolescence, or early adulthood.[9,27] Many mutation carriers may in fact be asymptomatic. The 2 probands we described seem to be affected by a very severe and life-threatening process.

At the molecular level, most *SCN5A* mutations associated with LQTS cause a subtle gain-of-function defect characterized by increased persistent current.[16,17] The markedly abnormal channel function we observed for G1631D including a 10-fold slowing of inactivation, substantial shifts in voltage dependence of activation and inactivation along with greatly impaired recovery from inactivation represent distinct molecular defects that distinguish this mutation from typical LQT3 alleles. Other *SCN5A* alleles may similarly predispose to early onset and severe perinatal arrhythmia syndromes,[4,5,28,29] but the functional aberrations associated with most of these reported alleles resemble mutations found in older individuals.

Negative Selection Against *SCN5A* Mutations

Mutations in *SCN5A* are represented disproportionately among SIDS victims who carry occult congenital arrhythmia susceptibility gene mutations when compared with older LQTS subjects. The lower proportion of *SCN5A* mutations among older children and young adults with LQTS when compared with the higher proportion in SIDS victims may be the result of negative selection against mutations in the sodium channel gene. Negative selection would cause an ascertainment bias for genotypes in living individuals in whom survival is favored when carrying mutations having less severe physiological consequences. In the case of SCN5A-G1631D, we assumed that without immediate treatment, this mutation would have been lethal. However, survival after successful treatment confounds the argument for negative selection.

Congenital arrhythmia susceptibility occurring in the perinatal and neonatal periods caused by *SCN5A* mutations appears biologically distinct from LQTS in older subjects. Carriers of certain *SCN5A* mutations may present with earlier onset and severe congenital arrhythmia syndromes. An illustration of this idea is recurrent third-trimester fetal loss attributable to inheritance of an *SCN5A* mutation (R1623Q) from a mother who was mosaic for this deleterious allele.[8] The R1623Q mutation, which affects a conserved residue in the D4/S4 segment nearby the location of G1631D, was originally identified in a Japanese child with a severe clinical presentation of LQTS,[30] and the molecular defect associated with this allele compromised inactivation to a greater extent than typical LQT3 mutations.[31] Our observations regarding the severity of biophysical defects associated with G1631D also support the idea that earlier onset cardiac symptoms may sometimes correlate with a severe molecular phenotype.

Genotype-Specific Pharmacological Treatment

The clinical consequences of G1631D were perinatal arrhythmias successfully managed in part by pharmacotherapy with the combination of mexiletine and propranolol. Mexiletine as well as other sodium channel blockers have been proposed as gene-specific therapeutic agents in LQT3.[32–34] In vitro studies have demonstrated the capability of these drugs to selectively suppress increased persistent current conducted by mutant channels[29,35] and to normalize ventricular repolarization in animal models.[36,37] One study suggested that certain biophysical properties of mutant $Na_v1.5$ channels may be predictive of mexiletine responsiveness. Specifically, Ruan et al[38] found that among 4 distinct *SCN5A* mutations, clinical benefit from mexiletine treatment was observed only in subjects carrying mutations that caused a hyperpolarizing shift in steady-state inactivation and this correlated with in vitro effects of the drug. However, this observation cannot be extrapolated to all *SCN5A* mutations as evidenced by the favorable response of G1631D to mexiletine both clinically and experimentally despite a depolarizing shift in steady-state inactivation (Figure 3). Similarly, another recently reported *SCN5A* mutation (F1473C) was also associated with a favorable clinical response to high-dose mexiletine despite having depolarized steady-state inactivation.[29] Additional factors besides those emphasized by Ruan et al[38] are likely to determine the clinical efficacy of mexiletine.

By contrast, use of β-blockers in the setting of *SCN5A* mutations has less certain benefits. Three studies have reported that β-blockers are generally less efficacious in LQT3 subjects, but the specific drug used varies considerably.[9,39,40] For example, in the report by Priori et al[40] the specific β-blocker was known in 69% of cases, and this was either propranolol or nadolol. As we have demonstrated in this study, propranolol may offer specific advantages in treating certain *SCN5A* mutations because of apparent local anesthetic-like properties of the drug.[18,19] By contrast, we recently determined that nadolol has no activity against sodium channels (Wang DW, unpublished observations, 2007). The role of propranolol in treating individuals with *SCN5A* mutations warrants further study.

Combination pharmacotherapy in the 2 probands with G1631D may have uniquely contributed to their survival. In the Japanese newborn, mexiletine alone was not adequate to control ventricular arrhythmia despite shortening of the QT interval. The addition of propranolol to the treatment regimen conferred better arrhythmia control and survival. In the Italian

proband, the coadministration of mexiletine with propranolol was efficacious, but this subject was also treated with ventricular pacing. Our study demonstrated additive effects of the 2 drugs at a pulsing frequency of 2 Hz (Figure 8). This observation suggested that a combination of mexiletine with propranolol in the setting of modest tachycardia were protective of ventricular arrhythmia caused by G1631D. We explain this effect by a combination of the intrinsic activity-dependent loss of channel availability observed for G1631D (Figure 4B) with the use-dependent drug effects.

Acknowledgments

The authors thank Thomas H. Rhodes for providing technical support and Shuji Hashimoto in the Laboratory of Clinical Physiology, National Cardiovascular Center, for technical assistance for MCG recordings.

Sources of Funding

This work was supported by a grant from the NIH (HL083374). Dr Shimizu was supported by a health sciences research grant (H18—Research on Human Genome—002) from the Ministry of Health, Labor, and Welfare, Japan.

Disclosures

None.

References

1. Byard RW, Krous HF. Sudden infant death syndrome: overview and update. *Pediatr Dev Pathol*. 2003;6:112–127.
2. Rognum TO, Byard RW. Sudden infant death syndrome, etiology and epidemiology. In: Payne-James J, Byard RW, Corey TS, Henderson C, eds. *Encyclopedia of Forensic and Legal Medicine*. Boston: Elsevier; 2005:117–129.
3. Arnestad M, Crotti L, Rognum TO, Insolia R, Pedrazzini M, Ferrandi C, Vege A, Wang DW, Rhodes TE, George AL Jr, Schwartz PJ. Prevalence of long-QT syndrome gene variants in sudden infant death syndrome. *Circulation*. 2007;115:361–367.
4. Wedekind H, Smits JP, Schulze-Bahr E, Arnold R, Veldkamp MW, Bajanowski T, Borggrefe M, Brinkmann B, Warnecke I, Funke H, Bhuiyan ZA, Wilde AA, Breithardt G, Haverkamp W. De novo mutation in the SCN5A gene associated with early onset of sudden infant death. *Circulation*. 2001;104:1158–1164.
5. Chang CC, Acharfi S, Wu MH, Chiang FT, Wang JK, Sung TC, Chahine M. A novel SCN5A mutation manifests as a malignant form of long QT syndrome with perinatal onset of tachycardia/bradycardia. *Cardiovasc Res*. 2004;64:268–278.
6. Lupoglazoff JM, Denjoy I, Villain E, Fressart V, Simon F, Bozio A, Berthet M, Benammar N, Hainque B, Guicheney P. Long QT syndrome in neonates: conduction disorders associated with HERG mutations and sinus bradycardia with KCNQ1 mutations. *J Am Coll Cardiol*. 2004;43:826–830.
7. Schwartz PJ, Priori SG, Dumaine R, Napolitano C, Antzelevitch C, Stramba-Badiale M, Richard TA, Berti MR, Bloise R. A molecular link between the sudden infant death syndrome and the long-QT syndrome. *N Engl J Med*. 2000;343:262–267.
8. Miller TE, Estrella E, Myerburg RJ, Garcia d V, Moreno N, Rusconi P, Ahearn ME, Baumbach L, Kurlansky P, Wolff G, Bishopric NH. Recurrent third-trimester fetal loss and maternal mosaicism for long-QT syndrome. *Circulation*. 2004;109:3029–3034.
9. Schwartz PJ, Priori SG, Spazzolini C, Moss AJ, Vincent GM, Napolitano C, Denjoy I, Guicheney P, Breithardt G, Keating MT, Towbin JA, Beggs AH, Brink P, Wilde AA, Toivonen L, Zareba W, Robinson JL, Timothy KW, Corfield V, Wattanasirichaigoon D, Corbett C, Haverkamp W, Schulze-Bahr E, Lehmann MH, Schwartz K, Coumel P, Bloise R. Genotype-phenotype correlation in the long-QT syndrome: gene-specific triggers for life-threatening arrhythmias. *Circulation*. 2001;103:89–95.
10. Tester DJ, Will ML, Haglund CM, Ackerman MJ. Compendium of cardiac channel mutations in 541 consecutive unrelated patients referred for long QT syndrome genetic testing. *Heart Rhythm*. 2005;2:507–517.
11. Priori SG, Schwartz PJ, Napolitano C, Bloise R, Ronchetti E, Grillo M, Vicentini A, Spazzolini C, Nastoli J, Bottelli G, Folli R, Cappelletti D. Risk stratification in the long-QT syndrome. *N Engl J Med*. 2003;348:1866–1874.
12. Crotti L, Lundquist AL, Insolia R, Pedrazzini M, Ferrandi C, De Ferrari GM, Vicentini A, Yang P, Roden DM, George AL Jr, Schwartz PJ. KCNH2-K897T is a genetic modifier of latent congenital long-QT syndrome. *Circulation*. 2005;112:1251–1258.
13. Yokokawa M, Noda T, Okamura H, Satomi K, Suyama K, Kurita T, Aihara N, Kamakura S, Shimizu W. Comparison of long-term follow-up of electrocardiographic features in Brugada syndrome between the SCN5A-positive probands and the SCN5A-negative probands. *Am J Cardiol*. 2007;100:649–655.
14. Catterall WA. Cellular and molecular biology of voltage-gated sodium channels. *Physiologic Rev*. 1992;72:S15–S48.
15. Chahine M, George AL Jr, Zhou M, Ji S, Sun W, Barchi RL, Horn R. Sodium channel mutations in paramyotonia congenita uncouple inactivation from activation. *Neuron*. 1994;12:281–294.
16. Bennett PB, Yazawa K, Makita N, George AL Jr. Molecular mechanism for an inherited cardiac arrhythmia. *Nature*. 1995;376:683–685.
17. Dumaine R, Wang Q, Keating MT, Hartmann HA, Schwartz PJ, Brown AM, Kirsch GE. Multiple mechanisms of Na^+ channel-linked long-QT syndrome. *Circ Res*. 1996;78:916–924.
18. Dawson AK, Reele SB, Wood AJ, Duff HJ, Woosley RL, Smith RF. Electrophysiological effects of high-dose propranolol in dogs: evidence in vivo for effects not mediated by the β adrenoceptor. *J Pharmacol Exp Ther*. 1984;229:91–97.
19. Duff HJ, Roden DM, Brorson L, Wood AJ, Dawson AK, Primm RK, Oates JA, Smith RF, Woosley RL. Electrophysiologic actions of high plasma concentrations of propranolol in human subjects. *J Am Coll Cardiol*. 1983;2:1134–1140.
20. Strasburger JF, Cheulkar B, Wichman HJ. Perinatal arrhythmias: diagnosis and management. *Clin Perinatol*. 2007;34:627–652.
21. Berul CI. Neonatal long QT syndrome and sudden cardiac death. *Prog Pediatr Cardiol*. 2000;11:47–54.
22. Schwartz PJ. Stillbirths, sudden infant deaths, and long-QT syndrome: puzzle or mosaic, the pieces of the jigsaw are being fitted together. *Circulation*. 2004;109:2930–2932.
23. Ackerman MJ, Siu BL, Sturner WQ, Tester DJ, Valdivia CR, Makielski JC, Towbin JA. Postmortem molecular analysis of SCN5A defects in sudden infant death syndrome. *JAMA*. 2001;286:2264–2269.
24. Brugada R, Hong K, Dumaine R, Cordeiro J, Gaita F, Borggrefe M, Menendez TM, Brugada J, Pollevick GD, Wolpert C, Burashnikov E, Matsuo K, Wu YS, Guerchicoff A, Bianchi F, Giustetto C, Schimpf R, Brugada P, Antzelevitch C. Sudden death associated with short-QT syndrome linked to mutations in HERG. *Circulation*. 2004;109:30–35.
25. Rhodes TE, Abraham RA, Welch RC, Vanoye CG, Crotti L, Arnestad M, Insolia R, Pedrazzini M, Ferrandi C, Vege A, Rognum T, Roden DM, Schwartz PJ, George AL Jr. Cardiac potassium channel dysfunction in sudden infant death syndrome. *J Mol Cell Cardiol*. 2007;44:571–581.
26. Tester DJ, Spoon DB, Valdivia HH, Makielski JC, Ackerman MJ. Targeted mutational analysis of the RyR2-encoded cardiac ryanodine receptor in sudden unexplained death: a molecular autopsy of 49 medical examiner/coroner's cases. *Mayo Clin Proc*. 2004;79:1380–1384.
27. Roden DM. Clinical practice. Long-QT syndrome. *N Engl J Med*. 2008;358:169–176.
28. Schulze-Bahr E, Fenge H, Etzrodt D, Haverkamp W, Monnig G, Wedekind H, Breithardt G, Kehl HG. Long QT syndrome and life threatening arrhythmia in a newborn: molecular diagnosis and treatment response. *Heart*. 2004;90:13–16.
29. Bankston JR, Yue M, Chung W, Spyres M, Pass RH, Silver E, Sampson KJ, Kass RS. A novel and lethal de novo LQT-3 mutation in a newborn with distinct molecular pharmacology and therapeutic response. *PLoS ONE*. 2007;2:e1258.
30. Yamagishi H, Furutani M, Kamisago M, Morikawa Y, Kojima Y, Hino Y, Furutani Y, Kimura M, Imamura S, Takao A, Momma K, Matsuoka R. A de novo missense mutation (R1623Q) of the SCN5A gene in a Japanese girl with sporadic long QT sydrome. *Hum Mutat*. 1998;11:481.
31. Kambouris NG, Nuss HB, Johns DC, Tomaselli GF, Marban E, Balser JR. Phenotypic characterization of a novel long-QT syndrome mutation (R1623Q) in the cardiac sodium channel. *Circulation*. 1998;97:640–644.
32. Schwartz PJ, Priori SG, Locati EH, Napolitano C, Cantu F, Towbin JA, Keating MT, Hammoude H, Brown AM, Chen LS. Long QT syndrome patients with mutations of the SCN5A and HERG genes have differential

responses to Na^+ channel blockade and to increases in heart rate. Implications for gene-specific therapy. *Circulation*. 1995;92:3381–3386.
33. Benhorin J, Taub R, Goldmit M, Kerem B, Kass RS, Windman I, Medina A. Effects of flecainide in patients with new SCN5A mutation: mutation-specific therapy for long-QT syndrome? *Circulation*. 2000;101:1698–1706.
34. Windle JR, Geletka RC, Moss AJ, Zareba W, Atkins DL. Normalization of ventricular repolarization with flecainide in long QT syndrome patients with SCN5A:ΔKPQ mutation. *Ann Noninvasive Electrocardiol*. 2001;6:153–158.
35. Wang DW, Yazawa K, Makita N, George AL Jr, Bennett PB. Pharmacological targeting of long QT mutant sodium channels. *J Clin Invest*. 1997;99:1714–1720.
36. Shimizu W, Aiba T, Antzelevitch C. Specific therapy based on the genotype and cellular mechanism in inherited cardiac arrhythmias: Long QT syndrome and Brugada syndrome. *Curr Pharm Des*. 2005;11:1561–1572.
37. Shimizu W, Antzelevitch C. Sodium channel block with mexiletine is effective in reducing dispersion of repolarization and preventing torsade des pointes in LQT2 and LQT3 models of the long-QT syndrome. *Circulation*. 1997;96:2038–2047.
38. Ruan Y, Liu N, Bloise R, Napolitano C, Priori SG. Gating properties of SCN5A mutations and the response to mexiletine in long-QT syndrome type 3 patients. *Circulation*. 2007;116:1137–1144.
39. Moss AJ, Zareba W, Hall WJ, Schwartz PJ, Crampton RS, Benhorin J, Vincent GM, Locati EH, Priori SG, Napolitano C, Medina A, Zhang L, Robinson JL, Timothy K, Towbin JA, Andrews ML. Effectiveness and limitations of β-blocker therapy in congenital long-QT syndrome. *Circulation*. 2000;101:616–623.
40. Priori SG, Napolitano C, Schwartz PJ, Grillo M, Bloise R, Ronchetti E, Moncalvo C, Tulipani C, Veia A, Bottelli G, Nastoli J. Association of long QT syndrome loci and cardiac events among patients treated with β-blockers. *JAMA*. 2004;292:1341–1344.

CLINICAL PERSPECTIVE

Mutations in *SCN5A* encoding the cardiac voltage-gated sodium channel have been associated with a spectrum of increased sudden death risk extending from fetal life to adulthood. We studied the functional and pharmacological properties of a novel de novo *SCN5A* mutation associated with an extremely severe perinatal presentation of congenital long-QT syndrome, characterized by late third trimester intrauterine fetal heart rhythm disturbances and life-threatening ventricular arrhythmia occurring within hours of emergency cesarean birth. The same mutation (G1631D), which was discovered in two subjects of different ethnic backgrounds with the same clinical presentation, caused a profound degree of sodium channel dysfunction that was more severe than that observed for any previous *SCN5A* variant. Despite the extreme nature of the mutation and the associated dire clinical scenario, the subjects survived owing to prompt therapeutic interventions, including treatment with the combination of mexiletine and propranolol, two drugs that exhibited enhanced and additive activity against the mutant allele. These observations illustrate the role of severe sodium channel mutations in a malignant perinatal variant of long-QT syndrome and successful use of combination pharmacotherapy to prevent perinatal mortality in this setting. Our data also illustrate the potential therapeutic benefits of a propranolol block of mutant sodium channels.

Journal of the American College of Cardiology
© 2008 by the American College of Cardiology Foundation
Published by Elsevier Inc.

Vol. 52, No. 16, 2008
ISSN 0735-1097/08/$34.00
doi:10.1016/j.jacc.2008.07.013

A Novel *SCN5A* Gain-of-Function Mutation M1875T Associated With Familial Atrial Fibrillation

Takeru Makiyama, MD, PHD,* Masaharu Akao, MD, PHD,* Satoshi Shizuta, MD,* Takahiro Doi, MD,* Kei Nishiyama, MD,* Yuko Oka, MD,† Seiko Ohno, MD, PHD,* Yukiko Nishio, MD,* Keiko Tsuji, MS,† Hideki Itoh, MD, PHD,† Takeshi Kimura, MD, PHD,* Toru Kita, MD, PHD,* Minoru Horie, MD, PHD†

Kyoto and Otsu, Japan

Objectives This study describes a novel heterozygous gain-of-function mutation in the cardiac sodium (Na^+) channel gene, *SCN5A*, identified in a Japanese family with lone atrial fibrillation (AF).

Background *SCN5A* mutations have been associated with a variety of inherited arrhythmias, but the gain-of-function type modulation in *SCN5A* is associated with only 1 phenotype, long-QT syndrome type 3 (LQTS3).

Methods We studied a Japanese family with autosomal dominant hereditary AF, multiple members of which showed an onset of AF or frequent premature atrial contractions at a young age.

Results The 31-year-old proband received radiofrequency catheter ablation, during which time numerous ectopic firings and increased excitability throughout the right atrium were documented. Mutational analysis identified a novel missense mutation, M1875T, in *SCN5A*. Further investigations revealed the familial aggregation of this mutation in all of the affected individuals. Functional assays of the M1875T Na^+ channels using a whole-cell patch-clamp demonstrated a distinct gain-of-function type modulation; a pronounced depolarized shift (+16.4 mV) in $V_{1/2}$ of the voltage dependence of steady-state inactivation; and no persistent Na^+ current, which is a defining mechanism of LQTS3. These biophysical features of the mutant channels are potentially associated with increased atrial excitability and normal QT interval in all of the affected individuals.

Conclusions We identified a novel *SCN5A* mutation associated with familial AF. The mutant channels displayed a gain-of-function type modulation of cardiac Na^+ channels, which is a novel mechanism predisposing to increased atrial excitability and familial AF. This is a new phenotype resulting from the *SCN5A* gain-of-function mutations and is distinct from LQTS3. (J Am Coll Cardiol 2008;52:1326–34) © 2008 by the American College of Cardiology Foundation

The cardiac sodium (Na^+) channel plays a crucial role in cardiac excitation/contraction via initiating the action potential of the conduction system and working myocytes. Mutations in *SCN5A*—which encodes the α-subunit of voltage-gated cardiac Na^+ channels—have been associated with a variety of cardiac arrhythmias. The loss-of-function mutations result in Brugada syndrome (1), idiopathic ventricular fibrillation (2), cardiac conduction disease (3), or congenital sick sinus syndrome (4), whereas the gain-of-function type modulation in *SCN5A* is associated with only 1 phenotype, long-QT syndrome type 3 (LQTS3) (5).

We reported on the screening for *SCN5A* mutations in Japanese patients with Brugada syndrome (6) and now have extended the cohort to various inherited arrhythmias, given the wide spectrum of clinical phenotypes of cardiac Na^+ channelopathies. In the present study, in a Japanese family with lone atrial fibrillation (AF), we identified a novel missense mutation of *SCN5A* (M1875T). Until recently, only potassium channel mutations have been linked to familial AF (7–10); however, 3 recent reports have identified *SCN5A* loss-of-function mutations: D1275N in 2 families with atrial arrhythmias (AF, cardiac conduction disease, or sick sinus syndrome) plus dilated cardiomyopathy (11,12), and N1986K in a family with lone AF (13). Thus, this is the first report to identify an *SCN5A* gain-of-function type mutation in familial AF.

From the *Department of Cardiovascular Medicine, Kyoto University Graduate School of Medicine, Kyoto, Japan; and the †Department of Cardiovascular and Respiratory Medicine, Shiga University of Medical Science, Otsu, Japan. This work was supported by research grants from the Japan Heart Foundation/Pfizer Japan Inc. Grant for Research on Cardiovascular Disease; Grants-in-Aid in Scientific Research from the Ministry of Education, Culture, Science, and Technology of Japan; and a Health Sciences Research Grant (H18-Research on human Genome-002) from the Ministry of Health, Labor and Welfare of Japan.

Manuscript received March 3, 2008; revised manuscript received July 7, 2008, accepted July 10, 2008.

Methods

Clinical evaluation. This study was approved by the Institutional Ethics Committee, and all patients provided informed consent. Affected individuals were considered as having AF or premature atrial contractions (PACs) when documented by 12-lead electrocardiograms (ECGs). Lone AF was defined as onset of AF at age <65 years without structural heart disease, hypertension, hyperthyroidism, myocardial infarction, or congestive heart failure. Paroxysmal AF was defined as sporadic AF lasting >30 s for <7 days. When sustained beyond 7 days, AF was considered persistent. Atrial fibrillation refractory to cardioversion or not attempted was classified as permanent. In both sinus rhythm and AF, the mean QT and RR intervals were measured from 3 and 6 consecutive beats, respectively.

Deoxyribonucleic acid (DNA) isolation and mutation analysis. Genomic DNA was isolated from blood lymphocytes and screened for candidate genes by denaturing high-performance liquid chromatography with a WAVE System Model 3500 (Transgenomic, Omaha, Nebraska). Abnormal conformers were amplified by polymerase chain reaction, and sequencing was performed on an ABI PRISM 3100 DNA sequencer (Applied Biosystems, Foster City, California).

Site-directed mutagenesis and electrophysiology. To construct the *SCN5A* mutant, we adopted site-directed mutagenesis performed via a kit, QuickChange II XL (Stratagene, La Jolla, California). The human cell line HEK293 cultured in a 35-mm dish was transiently transfected with 0.5 μg of either pRcCMV-WT or mutant complementary DNA in combination with 0.5 μg of the bicistronic plasmid (pEGFP-IRES-hβ1) encoding enhanced green fluorescent protein and the human β1-subunit (hβ1). The Na^+ currents were recorded 48 h after transfection with the whole-cell patch-clamp technique at 22°C to 23°C as described elsewhere (14). Results are expressed as mean ± SEM, and statistical significance was established with the Student *t* test. Statistical significance was assumed for $p < 0.05$.

Abbreviations and Acronyms

AF = atrial fibrillation
AT = atrial tachycardia
ECG = electrocardiogram
LQTS3 = long-QT syndrome type 3
PAC = premature atrial contraction
WT = wild-type

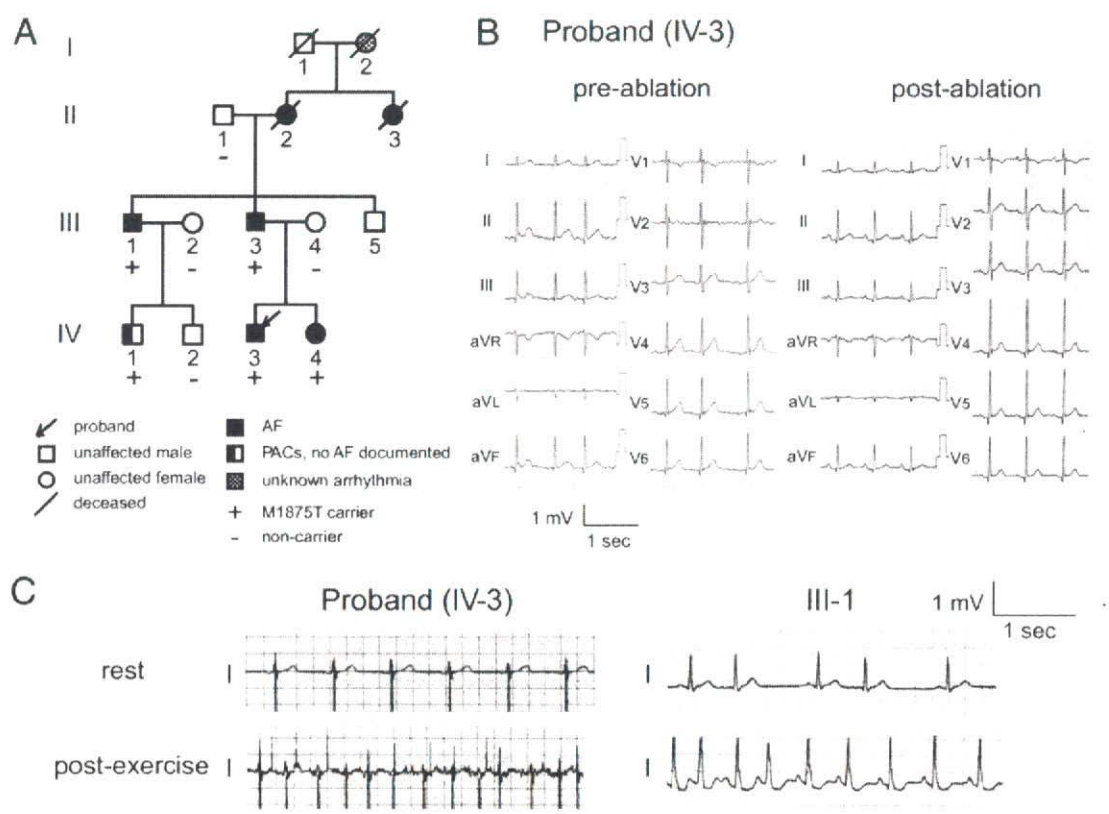

Figure 1 Pedigree and Clinical Features

(A) Pedigree of the family. Phenotypic traits are designated within pedigree symbols. **(B)** Electrocardiograms (ECGs) obtained from the proband, IV-3, before (**left panel**, atrial fibrillation [AF]) and after (**right panel**, sinus rhythm) he underwent radiofrequency catheter ablation. **(C)** At rest and post-exercise ECGs recorded from the proband (IV-3) and his uncle (III-1). Exercise-induced AF for the proband and atrial tachycardia for the uncle can be observed. *Continued on next page.*

JACC Vol. 52, No. 16, 2008
October 14, 2008:1326–34

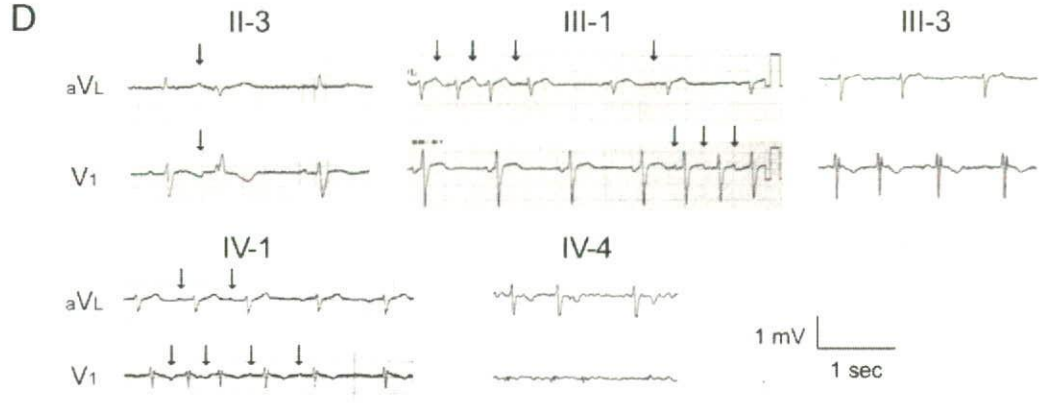

Figure 1 Continued

(D) Electrocardiograms recorded from other affected individuals. **Arrows** indicate P waves of premature atrial contractions (PACs) in II-3, III-1, and IV-1. III-3 and IV-4 demonstrated AF.

Results

Clinical features. We studied a Japanese family with autosomal dominant hereditary AF that spanned 3 generations (Fig. 1A). The proband (IV-3) (Fig. 1A), a 31-year-old man, first experienced repetitive palpitation due to frequent PACs at age 18, which later progressed to paroxysmal AF and atrial tachycardia (AT) at age 27 years (pre-ablation) (Fig. 1B).

Six family members, along with the proband, presented with either AF or frequent PACs (Fig. 1A). The majority shared a similar clinical course with the proband—palpitations due to PACs start in their teens, which later progress to paroxysmal and ultimately persistent AF (Table 1). The proband and his uncle (III-1) showed exercise-induced AT and/or AF (Fig. 1C). The proband's cousin (IV-1) presented with frequent PACs (Fig. 1D) that have not yet progressed to AF. The ECGs of the affected relatives—with the exception to the proband's aunt (II-3), who received disopyramide—did not show any QT prolongation (Fig. 1D, Table 1). Interestingly, the analysis of P wave morphology in the affected family members revealed that the majority of PAC foci were localized in the right atrium (Fig. 1D). The affected individuals received various antiarrhythmic agents (Table 1) but, in most cases, to no avail. There was neither structural heart disease nor a history of major ventricular arrhythmias or sudden cardiac death in this family.

At age 27 years, the proband underwent radiofrequency catheter ablation. Intravenous administration of isoproterenol induced repetitive ATs from multiple origins in the right atrium (Fig. 2A). We successfully ablated the major origin, located in the lower-right atrial septum (Figs. 2B and 2C).

Three years later, the second ablation session was performed due to a relapse of persistent AF. This time, we identified 2 other PAC foci in the right atrium (Fig.

Table 1 Clinical Characteristics of Affected Individuals

Individual	Gender	Age (yrs)	Arrhythmias	Onset of PAC (yrs)	Onset of AF (yrs)	Mutation Carrier	HR (beats/min)	QRS (ms)	QTc	LAD (mm)	LVEF (%)	Antiarrhythmic Agents Used to Treat AF
I-2	F	90*	Unknown	NA	NA	ND	NA	NA	NA	NA	NA	NA
II-2	F	75*	Permanent AF	NA	NA	ND	88	74	427	36	79	—
II-3	F	75*	Paroxysmal AF, PACs	NA	NA	ND	77†	104†	478†	30	75	Disopyramide
III-1	M	60	Paroxysmal AF, PACs	NA	48	Yes	70	92	394	32	75	Disopyramide, cibenzoline, aprindine
III-3	M	57	Permanent AF	15	51	Yes	71	82	385	NA	NA	—
IV-1	M	34	PACs	23	—	Yes	68	82	399	ND	ND	—
IV-3	M	31	Persistent AF	18	27	Yes	65	81	388	30	63	Pilsicainide, flecainide
IV-4	F	29	Permanent AF	12	26	Yes	88	87	429	31	61	Pilsicainide

*Age of death; †disopyramide administration.
AF = atrial fibrillation; HR = heart rate; LAD = left atrial dimension; LVEF = left ventricular ejection fraction; NA = records not available; ND = not determined; PAC = premature atrial contraction.

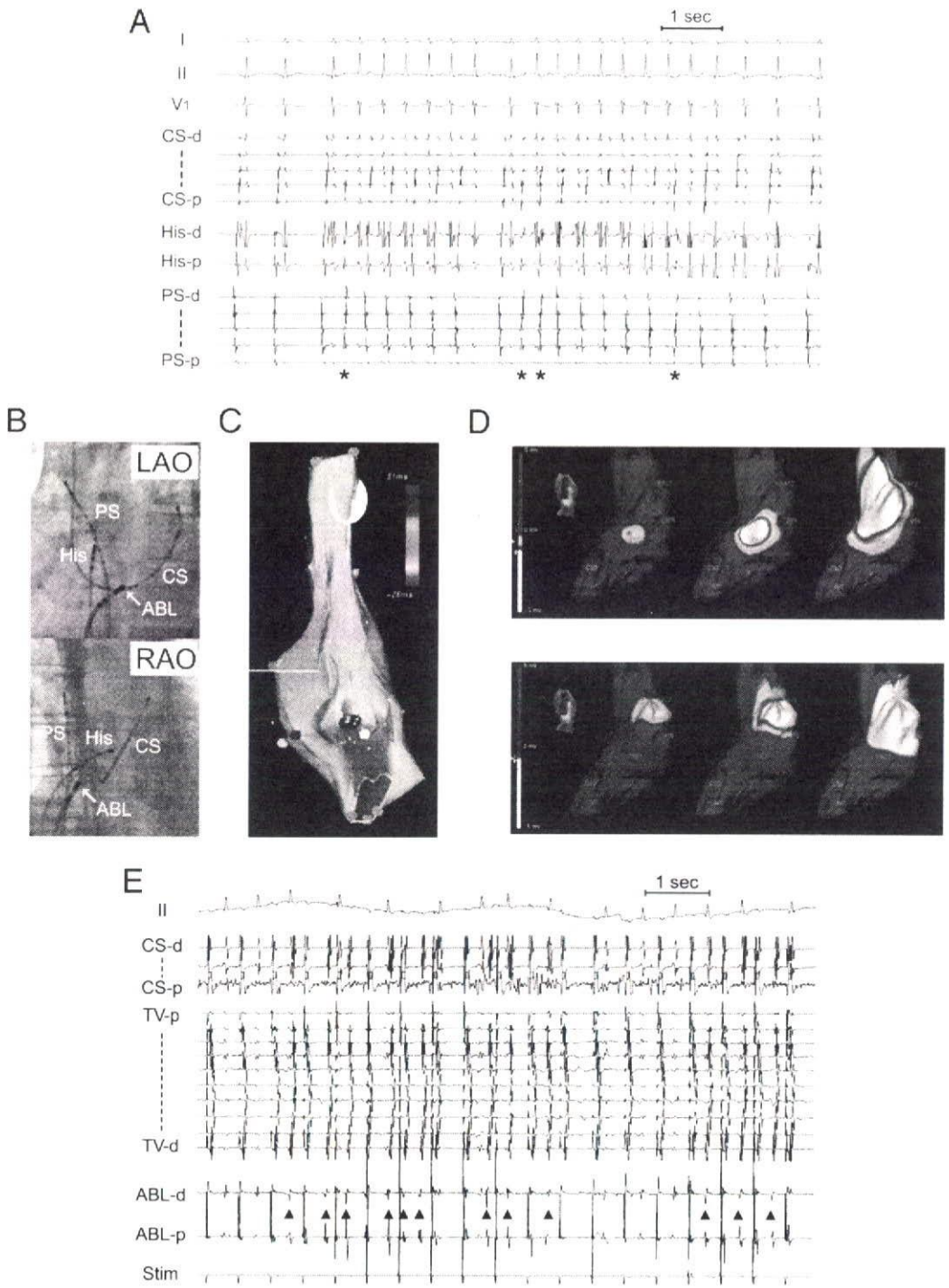

Figure 2 **Radiofrequency Catheter Ablation Recordings**

The first **(A to C)** and the second **(D and E)** ablation sessions on the proband. **(A)** Repetitive atrial tachycardias (ATs) from multiple origins. Shown are intracardiac recordings from the coronary sinus (CS), the His bundle (His), and a catheter placed along the posterior septum (PS) in the right atrium. Note that atrial activation sequences in CS during ATs were consistently proximal to distal, suggesting right atrial origins. **Asterisks** indicate the successfully ablated AT originating from the lower-right atrial septum. **(B)** Fluoroscopic images of the electrodes in the left anterior oblique (LAO) and right anterior oblique (RAO) views. Position of the ablation catheter (ABL; indicated by **arrows**); successful ablation site of the AT. **(C)** Three-dimensional electroanatomic map of the AT in the right posterior oblique view. The AT focus in the lower-right atrial septum was successfully ablated in the first session. **(D)** Noncontact mapping of PACs in the right lateral view. Two PAC foci in the middle of the crista terminalis **(upper panel)** and the high posterolateral wall **(lower panel)** ablated successfully in the second session are shown. **(E)** Numerous electrical firings (▲) from the contact site during radiofrequency energy delivery in generating tricuspid valve isthmus block. Continuous pacing was performed from proximal CS. Stim = stimulator; TV = tricuspid valve annulus; other abbreviations as in Figure 1.

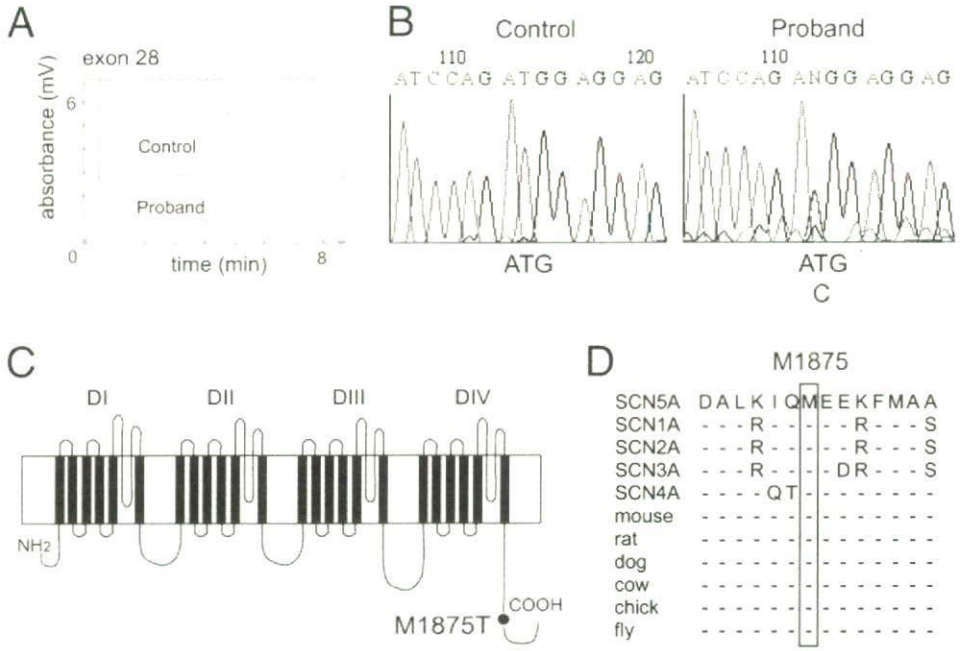

Figure 3 **Genetic Analysis**

(A) The denaturing high-performance liquid chromatography elution profiles for an *SCN5A* mutation, M1875T, detected in the affected family members. **(B)** Deoxyribonucleic acid sequencing electropherograms demonstrate heterozygosity for a *SCN5A* mutation. **(C)** Topology of the α-subunit of voltage-gated cardiac sodium (Na^+) channel. The location of the detected mutation is shown. **(D)** Amino acid sequence alignments of *SCN5A* with related Na^+ channels. The *SCN5A* indicates human heart; *SCN1A*, human brain type I; *SCN2A*, human brain type II; *SCN3A*, human brain type III; *SCN4A*, human skeletal muscle. The sequences of other species represent the cardiac isoforms of Na^+ channels.

2D)—both were successfully ablated. During the subsequent procedure to generate a cavotricuspid isthmus block, we noticed that energy delivery from the catheter induced numerous electrical firings from the contact sites (Fig. 2E). After the second ablation session, he maintained a sinus rhythm under medication, yet even after which he experienced occasional episodes of paroxysmal AF. Interestingly, after each attempt of cardioversion, ATs that lasted for several seconds were observed immediately after the shock was delivered and before sinus rhythm conversion (data not shown). All of these features strongly suggest the proband's increased vulnerability to atrial arrhythmias.

Genetic analysis. We identified a novel missense mutation, c.5624T>C, p.M1875T, in the *SCN5A* gene in the proband. Figure 3 shows the denaturing high-performance liquid chromatography and sequence results (Figs. 3A and 3B) and an illustration showing the position of the identified mutation (Fig. 3C). The amino acid at codon 1875 (methionine) is highly conserved among different Na^+ channel isoforms and species (Fig. 3D). Furthermore, this mutation was absent in 210 Japanese control individuals (420 chromosomes). We failed to identify mutations in any other potential candidate genes of familial AF (*KCNQ1*, *KCNH2*, *KCNE1*, *KCNE2*, *KCNE3*, *KCNJ2*, and *KCNA5*). Further analysis of the family members revealed that the M1875T mutation in SCN5A perfectly matched their clinical phenotypes (Figs. 1A and 1D, Table 1).

Functional analysis of M1875T-*SCN5A*. We performed biophysical assays for the novel *SCN5A* mutation with a heterologous expression system in HEK293 cells. Figure 4A illustrates representative whole-cell current traces from cells expressing wild-type (WT) and M1875T Na^+ channels in the presence of the coexpressed Na^+ channel β subunit.

Notably, M1875T channels showed an apparently slower inactivation compared with WT. The time constants for both fast and slow inactivation across a wide range of test potentials were significantly larger with M1875T in comparison with WT (Fig. 4B), indicating impaired inactivation. Figure 4C shows the peak current-voltage relation for WT and M1875T channels. The maximum current density of WT was observed at −20 mV but shifted to −30 mV for M1875T. In addition, the peak current density of M1875T was significantly larger than WT (WT, 326.2 ± 28.2 pA/pF, n = 23; M1875T, 484.6 ± 49.6 pA/pF, n = 31, $p < 0.01$) (Fig. 4D). As in WT, M1875T channels showed no persistent inward Na^+ currents at the end of a 200-ms depolarization (Fig. 4E), which is one of the defining mechanisms of QT interval prolongation in patients with LQTS3. The subtracted amplitude at the end of the 200-ms depolarization was 0.046 ± 0.009% (n = 5) of the peak current for WT and 0.048 ± 0.038% (n = 7) for M1875T.

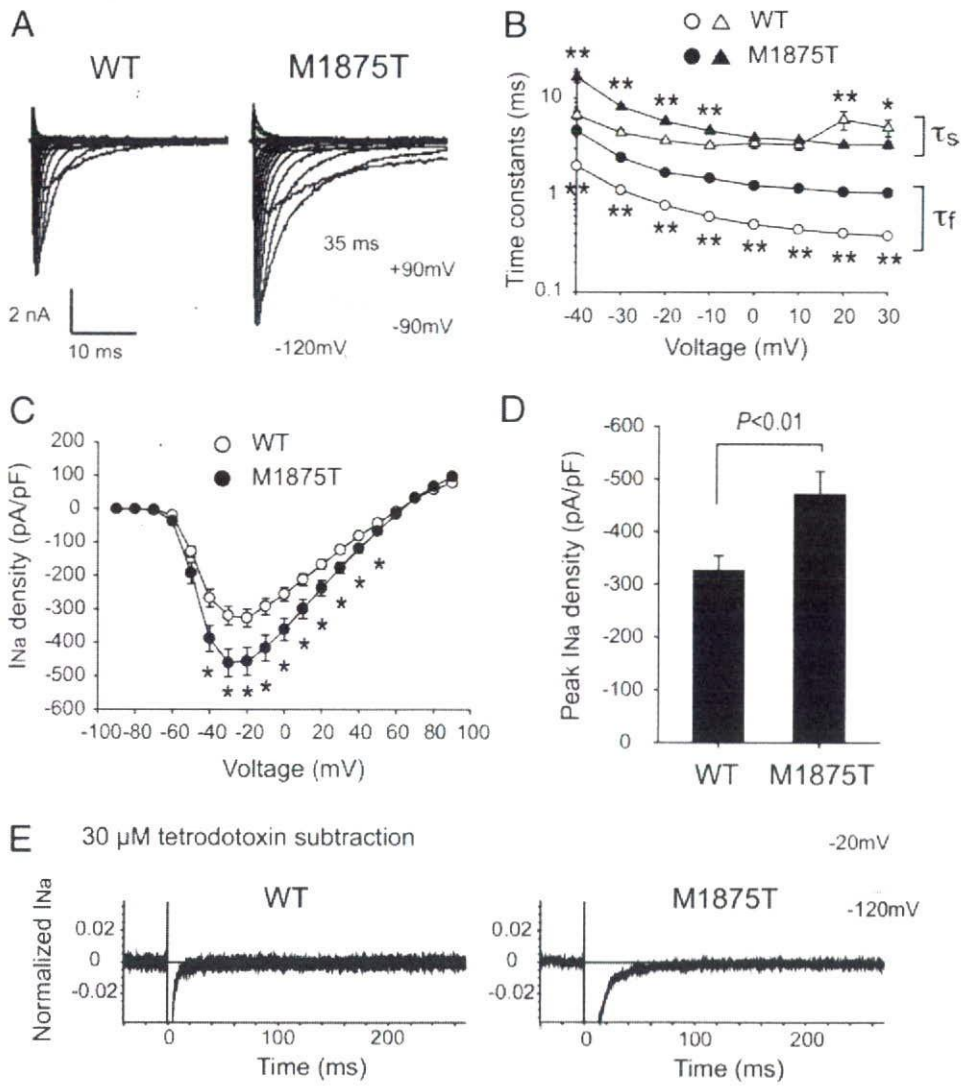

Figure 4 **Macroscopic Na^+ Currents of M1875T Channels**

(A) Representative whole-cell current traces of wild-type (WT) and M1875T sodium (Na^+) channels. Cells were transfected with human β1-subunit (protocol shown as an inset). **(B)** Voltage dependence of inactivation time constants. The time course of inactivation was fit with a 2 exponential equation: $I/I_{max} = A_f \times \exp(-t/\tau_f) + A_s \times \exp(-t/\tau_s)$. Lower and upper bundles of symbols indicate fast (τ_f) and slow (τ_s) time constant values, respectively. Statistically significant differences are indicated (*$p < 0.05$, **$p < 0.01$). **(C)** Average current-voltage relationship for WT and M1875T channels. The current is normalized to cell capacitance to give a measure of Na^+ current density. **Asterisks** indicate the voltages at which the current density was statistically different (*$p < 0.05$). **(D)** Average peak Na^+ current density of WT and M1875T channels. The peak current density was significantly larger in M1875T (WT at −20 mV, 326.2 ± 28.2 pA/pF, n = 23; M1875T at −30 mV, 484.6 ± 49.6 pA/pF, n = 31, $p < 0.05$). **(E)** Representative Na^+ current traces recorded in the absence or presence of 30 μmol/l tetrodotoxin. Tetrodotoxin-sensitive persistent currents were calculated by digital subtraction. M1875T channels showed no persistent inward Na^+ currents.

Figure 5A shows the conductance-voltage and steady-state inactivation curves for WT and M1875T channels. Numerical data pertaining to the biophysical properties therein are summarized in Table 2. The parameters for the activation gate were similar between WT and M1875T. In contrast, the half-maximal potential ($V_{1/2}$) for the steady-state inactivation of M1875T showed a marked positive shift (+16.4 mV) compared with that of WT (WT, $V_{1/2}$ = −78.08 ± 0.94 mV, n = 22; M1875T, $V_{1/2}$ = −61.68 ± 0.76 mV, n = 33, $p < 0.01$). The slope factor (k) for M1875T was significantly larger than that of WT (WT, k = −7.13 ± 0.12, n = 22; M1875T, k = −6.07 ± 0.16, n = 33, $p < 0.01$). The pronounced depolarizing shift of the inactivation gate is likely to increase Na^+ channel availability during excitation.

We also investigated the other kinetic properties of Na^+ channels: recovery from inactivation, onset of slow inactivation, and closed-state inactivation. Parameters of recovery from inactivation and onset of slow inactivation were identical between WT and M1875T (Figs. 5B and 5C,

Table 2 Biophysical Properties of WT and M1875T Channels

	WT	M1875T
Activation (mV)	(n = 23)	(n = 37)
$V_{1/2}$	−43.61 ± 0.79	−44.09 ± 0.72
k	6.53 ± 0.16	5.98 ± 0.18
Steady-state inactivation (mV)	(n = 22)	(n = 33)
$V_{1/2}$	−78.08 ± 0.94	−61.68 ± 0.76†
k	7.13 ± 0.12	6.07 ± 0.16†
Recovery from inactivation	(n = 16)	(n = 25)
A_f	0.84 ± 0.01	0.84 ± 0.01
A_s	0.15 ± 0.01	0.15 ± 0.01
τ_f (ms)	8.95 ± 0.95	8.32 ± 0.83
τ_s (ms)	338.6 ± 30.4	271.6 ± 31.6
Onset of slow inactivation	(n = 15)	(n = 16)
A	0.12 ± 0.01	0.12 ± 0.01
τ (ms)	773.9 ± 90.0	647.2 ± 70.6
Closed-state inactivation	(n = 9)	(n = 9)
A	0.13 ± 0.03	0.05 ± 0.02*
τ (ms)	97.1 ± 7.8	212.7 ± 22.3†

Data are mean ± SEM. Parameters were obtained from fitting individual experiments illustrated in Figure 4. *p < 0.05; †p < 0.01 versus wild-type (WT).

A and τ = fractional amplitude and time constant, respectively; n = number of tested cells; $V_{1/2}$ and k = midpoint potential and slope factor, respectively.

Table 2). With regard to closed-state inactivation, the extent was significantly less (WT, A = 0.13 ± 0.03 ms, n = 9; M1875T, A = 0.05 ± 0.02 ms, n = 9, $p < 0.05$), and the time constant was larger in the M1875T channels when compared with WT (WT, τ = 97.1 ± 7.8 ms, n = 9; M1875T, τ = 212.7 ± 22.3 ms, n = 9, $p < 0.01$) (Fig. 5D, Table 2). These data suggest that the number of inactivated M1875T channels is reduced near the resting potential.

Collectively, the M1875T mutation exhibited a gain-of-function type modulation in the cardiac Na^+ channels without persistent inward Na^+ currents: increased peak Na^+ channel density; prolonged time constants of both fast and slow inactivation; a large depolarizing shift in $V_{1/2}$ of the steady-state inactivation; and a lesser extent and a larger time constant with regard to closed-state inactivation. In short, the M1875T mutation clearly demonstrates characteristics that make it distinct from the LQTS3-type gain-of-function modulation.

Discussion

In the present study, we identified a novel gain-of-function *SCN5A* mutation that causes a familial form of AF. The clinical course of AF development materialized in a similar fashion among all affected family members (i.e., palpitations due to frequent PACs and ATs in their teens, followed by paroxysmal and then persistent AF). During the clinical electrophysiological study in the proband, we recognized multifocal activity sites and increased excitability in the right atrium. These distinguishing features are presumably associated with the unique biophysical properties of the mutant Na^+ channels. It should be noted, however, that the size of the pedigree analyzed in this study is limited.

***SCN5A* mutations and familial AF.** Mutations in *SCN5A* have been reported to cause a wide variety of cardiac arrhythmias. The gain-of-function mutations result in LQTS3 (5), whereas the loss-of-function mutations result in various phenotypes: 1) Brugada syndrome; 2) idiopathic ventricular fibrillation; 3) cardiac conduction disease; and 4) congenital sick sinus syndrome. We previously reported that *SCN5A*-linked Brugada syndrome is a high-risk group of bradyarrhythmias, linked predominantly to sick sinus syndrome (6). Although AF is a common complication of Brugada syndrome (10% to 30%) (6,15), there is a scarcity of reports on *SCN5A*-positive Brugada syndrome and AF.

Atrial fibrillation is the most common form of cardiac arrhythmia, characterized by rapid irregular activation of the atrium, and a common cause of morbidity and mortality. Atrial fibrillation occurs predominantly in elderly persons and is frequently associated with underlying cardiac diseases. In 15% to 30% of patients, however, an etiology is absent (i.e., lone AF) (16,17). Although AF has been regarded a sporadic and acquired disease, the familial aggregation of AF has been shown to be more frequent than previously recognized (18,19). Chen et al. (7) found the first gene mutation responsible for familial AF in *KCNQ1*, which encodes the α-subunit of slow delayed rectifier potassium (K^+) channels. Since then, 3 additional genes—all of which encode cardiac K^+ channels—responsible for familial AF have been identified: *KCNE2* (8), *KCNJ2* (9), and *KCNA5* (10). Recently, loss-of-function *SCN5A* mutations (D1275N) were reported to be associated with 2 families who have atrial arrhythmias (AF, cardiac conduction disease, and sick sinus syndrome) with dilated cardiomyopathy (11,12). More recently, an *SCN5A* mutation (N1986K) was identified in a family with lone AF (13). Functional assays on the N1986K channels revealed a hyperpolarized shift of steady-state inactivation, indicating a loss-of-function type modulation. One of the affected members underwent pacemaker implantation due to sick sinus syndrome, suggesting the underlying conduction disturbance resulting from the Na^+ channel loss-of-function. In addition, a common polymorphism (H558R) in *SCN5A*, present in 20% of the population (20), reduces Na^+ current density (21). The screening for the polymorphism in 157 patients with lone AF revealed that the R558 allele was more common in patients with lone AF than in the control subjects and as such was considered to be a risk factor for lone AF (22). However, none of the M1875T-positive individuals carried the R558 allele.

These reports implicate a potential relationship between decreased Na^+ currents and AF; however, to date, an *SCN5A* gain-of-function mutation has never been linked to AF.

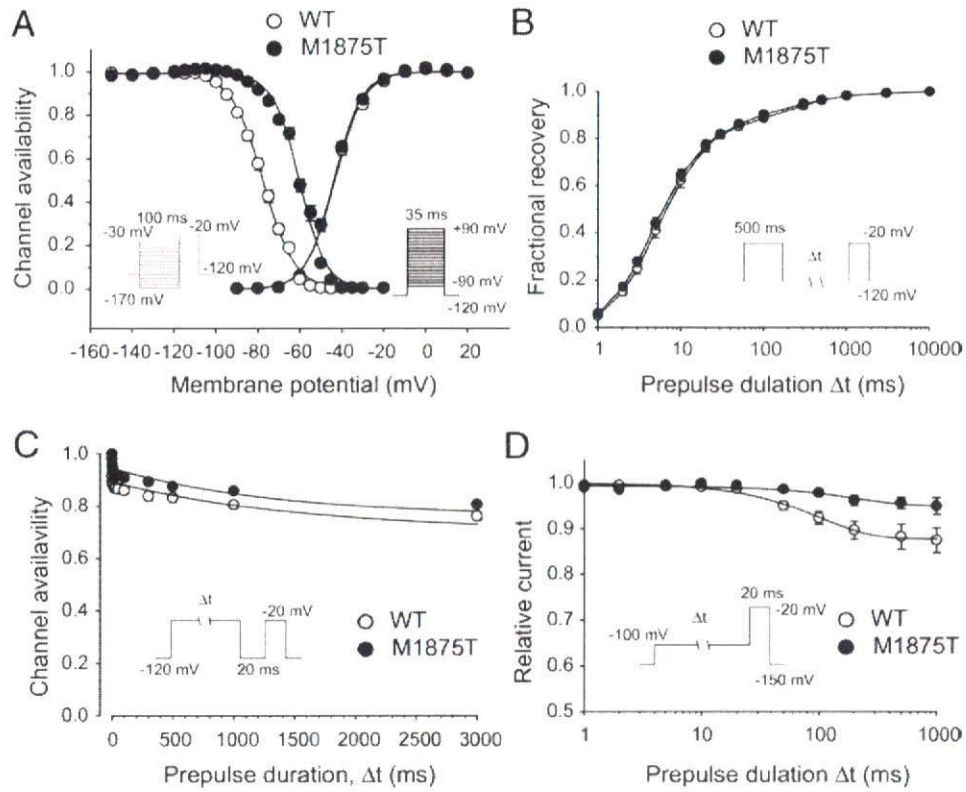

Figure 5 **Gating Properties for M1875T Channels**

Detailed parameters are given in Table 2. **(A)** Voltage dependence of relative sodium (Na^+) conductance activation and steady-state inactivation were determined by means of the voltage protocols, as shown in the inset. Curves were fit with the Boltzmann equation, $I/I_{max} = (1 + \exp[V-V_{1/2}]/k)^{-1}$ to determine the membrane potential for half-maximal inactivation or activation ($V_{1/2}$) and the slope factor k. Note that M1875T channels showed a pronounced depolarized shift (+16.4 mV) in the $V_{1/2}$ of steady-state inactivation compared with wild-type (WT). **(B)** Time course of recovery from inactivation was elicited with a double pulse protocol. Data were fit with a 2 exponential equation: $I/I_{max} = A_f \times (1 - \exp[-t/\tau_f]) + A_s \times (1 - \exp[-t/\tau_s])$, where A_f and A_s are fractions of fast and slow inactivation components, and τ_f and τ_s are the time constants of fast and slow inactivation components, respectively. **(C)** Onset of slow inactivation. Time course of entry into the slow inactivation state was obtained by a double pulse protocol. Curves were fit with a single exponential equation: $I/I_{max} = y0 + A \times \exp(-t/\tau)$. **(D)** Closed-state inactivation. The transfer rate of Na^+ channels from closed-state to inactivated closed-state without an intervening opening state was measured by a double pulse protocol. Time course for development of closed-state inactivation was fit with a single exponential equation: $I/I_{max} = y0 + A \times \exp(-t/\tau)$. The extent of closed-state inactivation was significantly less and the time constant larger in M1875T channels in comparison with WT.

Unique gain-of-function properties of M1875T Na^+ channels. To date, *SCN5A* gain-of-function mutations have been reportedly linked to only 1 phenotype, LQTS3. Persistent inward Na^+ currents observed in these mutant channels are considered to cause QT prolongation. However, M1875T channels did not display persistent inward Na^+ currents (Fig. 4E). This might explain why all of the affected and mutation-positive individuals in our study exhibited normal QT interval, with the exception of 1 individual who received disopyramide therapy. The functional properties of M1875T Na^+ channels were quite distinct from those of LQTS3. The most prominent change was a +16.4 mV shift in the steady-state inactivation. This is, to the best of our knowledge, the greatest depolarization shift in all of the previously reported SCN5A mutants. Some of the LQTS3 mutants (E1295K, A1330P, A1330T, and I1768V) showed a similar depolarizing shift of the steady-state inactivation without persistent inward Na^+ currents; however, the extent of the depolarizing shift was much less than M1875T (all were <+10 mV). The M1875T channels displayed the increased peak Na^+ current density (Fig. 4D), perhaps due to the large depolarized shift in steady-state inactivation. Interestingly, the location of the mutation is within a complex region that includes Ca^{2+} binding EF-hand like motifs and a putative binding site for calmodulin (23), and thus the mutation might disrupt inactivation by altered calcium sensitivity.

The potential mechanisms by which the identified gain-of-function mutation might lead to PAC or AF could be explained as the following: first, increased inward Na^+ currents might cause repolarization failure or early afterdepolarizations, thereby inducing triggered activities; and second, the increased Na^+ currents might increase the conduction velocity and facilitate the maintenance of the fibrillation wave. However, further studies are needed to elucidate the underlying mechanisms.

Genotype–phenotype relationship and clinical implications. Quite impressively, the affected family members shared a similar clinical course with high penetrance—frequent PACs and ATs first appeared during their teens and subsequently progressed to AF (Fig. 1A). Increased automaticity and irritability in the atrium was demonstrated by recurrent atrial arrhythmias that were resistant to ablation or drug therapy, induced PACs during exercise (Fig. 1C), and numerous ectopic firings and increased excitability throughout the right atrium during catheter ablation (Fig. 2). Because Na^+ channels encoded by *SCN5A* are expressed in both the atrium and ventricle, it remains unknown why our patients showed only atrial arrhythmias but not ventricular arrhythmias. The different electrophysiological properties between atrial and ventricular cells might be the underlying cause. Resting membrane potential is more depolarized, and the peak Na^+ current density is larger in atrial cells than in ventricular cells in dogs (24). The critical depolarization and current threshold for action potential initiation are smaller in atrial cells than in ventricular cells, indicating that atrial cells are more readily excitable than ventricular cells (25).

Conclusions

We identified a novel *SCN5A* gain-of-function mutation that causes a familial form of AF without any underlying structural heart diseases, which provides us with new insight into the pathogenesis of the commonly occurring form of AF.

Acknowledgment

The authors thank Richard Kaszynski for his critical reading of the manuscript.

Reprint requests and correspondence: Dr. Masaharu Akao, Department of Cardiovascular Medicine, Kyoto University Graduate School of Medicine, 54 Shogoin Kawahara-cho, Sakyo-ku, Kyoto, 606-8507, Japan. E-mail: akao@kuhp.kyoto-u.ac.jp.

REFERENCES

1. Chen Q, Kirsch GE, Zhang D, et al. Genetic basis and molecular mechanism for idiopathic ventricular fibrillation. Nature 1998;392:293–6.
2. Akai J, Makita N, Sakurada H, et al. A novel SCN5A mutation associated with idiopathic ventricular fibrillation without typical ECG findings of Brugada syndrome. FEBS Lett 2000;479:29–34.
3. Schott JJ, Alshinawi C, Kyndt F, et al. Cardiac conduction defects associate with mutations in SCN5A. Nat Genet 1999;23:20–1.
4. Benson DW, Wang DW, Dyment M, et al. Congenital sick sinus syndrome caused by recessive mutations in the cardiac sodium channel gene (SCN5A). J Clin Invest 2003;112:1019–28.
5. Wang Q, Shen J, Splawski I, et al. SCN5A mutations associated with an inherited cardiac arrhythmia, long QT syndrome. Cell 1995;80:805–11.
6. Makiyama T, Akao M, Tsuji K, et al. High risk for bradyarrhythmic complications in patients with Brugada syndrome caused by SCN5A gene mutations. J Am Coll Cardiol 2005;46:2100–6.
7. Chen YH, Xu SJ, Bendahhou S, et al. KCNQ1 gain-of-function mutation in familial atrial fibrillation. Science 2003;299:251–4.
8. Yang Y, Xia M, Jin Q, et al. Identification of a KCNE2 gain-of-function mutation in patients with familial atrial fibrillation. Am J Hum Genet 2004;75:899–905.
9. Xia M, Jin Q, Bendahhou S, et al. A Kir2.1 gain-of-function mutation underlies familial atrial fibrillation. Biochem Biophys Res Commun 2005;332:1012–9.
10. Olson TM, Alekseev AE, Liu XK, et al. Kv1.5 channelopathy due to KCNA5 loss-of-function mutation causes human atrial fibrillation. Hum Mol Genet 2006;15:2185–91.
11. McNair WP, Ku L, Taylor MRG, et al. SCN5A mutation associated with dilated cardiomyopathy, conduction disorder, and arrhythmia. Circulation 2004;110:2163–7.
12. Olson TM, Michels VV, Ballew JD, et al. Sodium channel mutations and susceptibility to heart failure and atrial fibrillation. JAMA 2005;293:447–54.
13. Ellinor PT, Nam EG, Shea MA, Milan DJ, Ruskin JN, Macrae CA. Cardiac sodium channel mutation in atrial fibrillation. Heart Rhythm 2008;5:99–105.
14. Shirai N, Makita N, Sasaki K, et al. A mutant cardiac sodium channel with multiple biophysical defects associated with overlapping clinical features of Brugada syndrome and cardiac conduction disease. Cardiovasc Res 2002;53:348–54.
15. Bordachar P, Reuter S, Garrigue S, et al. Incidence, clinical implications and prognosis of atrial arrhythmias in brugada syndrome. Eur Heart J 2004;25:879–84.
16. Murgatroyd FD, Camm AJ. Atrial arrhythmias. Lancet 1993;341:1317–22.
17. Levy S, Maarek M, Coumel P, et al. Characterization of different subsets of atrial fibrillation in general practice in France: the ALFA study. Circulation 1999;99:3028–35.
18. Darbar D, Herron KJ, Ballew JD, et al. Familial atrial fibrillation is a genetically heterogeneous disorder. J Am Coll Cardiol 2003;41:2185–92.
19. Ellinor PT, Yoerger DM, Ruskin JN, MacRae CA. Familial aggregation in lone atrial fibrillation. Hum Genet 2005;118:179–84.
20. Ackerman MJ, Splawski I, Makielski JC, et al. Spectrum and prevalence of cardiac sodium channel variants among black, white, Asian, and Hispanic individuals: implications for arrhythmogenic susceptibility and Brugada/long QT syndrome genetic testing. Heart Rhythm 2004;1:600–7.
21. Makielski JC, Ye B, Valdivia CR, et al. A ubiquitous splice variant and a common polymorphism affect heterologous expression of recombinant human SCN5A heart sodium channels. Circ Res 2003;93:821–8.
22. Chen LY, Ballew JD, Herron KJ, Rodeheffer RJ, Olson TM. A common polymorphism in SCN5A is associated with lone atrial fibrillation. Clin Pharmacol Ther 2007;81:35–41.
23. Deschenes I, Neyroud N, DiSilvestre D, Marban E, Yue DT, Tomaselli GF. Isoform-specific modulation of voltage-gated Na(+) channels by calmodulin. Circ Res 2002;90:E49–57.
24. Burashnikov A, Di Diego JM, Zygmunt AC, Belardinelli L, Antzelevitch C. Atrium-selective sodium channel block as a strategy for suppression of atrial fibrillation: differences in sodium channel inactivation between atria and ventricles and the role of ranolazine. Circulation 2007;116:1449–57.
25. Golod DA, Kumar R, Joyner RW. Determinants of action potential initiation in isolated rabbit atrial and ventricular myocytes. Am J Physiol Heart Circ Physiol 1998;274:H1902–13.

Key Words: arrhythmia ▪ atrial fibrillation ▪ genetics ▪ ion channels ▪ sodium.

Sodium channel β1 subunit mutations associated with Brugada syndrome and cardiac conduction disease in humans

Hiroshi Watanabe,[1,2] Tamara T. Koopmann,[3] Solena Le Scouarnec,[4,5,6] Tao Yang,[1] Christiana R. Ingram,[1] Jean-Jacques Schott,[4,5,6,7] Sophie Demolombe,[4,5,6] Vincent Probst,[4,5,6,7] Frédéric Anselme,[8] Denis Escande,[4,5,6,7] Ans C.P. Wiesfeld,[9] Arne Pfeufer,[10,11] Stefan Kääb,[12] H.-Erich Wichmann,[11,12] Can Hasdemir,[13] Yoshifusa Aizawa,[2] Arthur A.M. Wilde,[3] Dan M. Roden,[1] and Connie R. Bezzina[3]

[1]Department of Medicine and Pharmacology, Vanderbilt University School of Medicine, Nashville, Tennessee, USA. [2]Division of Cardiology, Niigata University Graduate School of Medical and Dental Sciences, Niigata, Japan. [3]Heart Failure Research Center, Department of Experimental Cardiology, Academic Medical Center, University of Amsterdam, Amsterdam, The Netherlands. [4]INSERM, UMR915, l'institut du thorax, Nantes, France. [5]Université de Nantes, Nantes, France. [6]CNRS ERL3147, Nantes, France. [7]CHU Nantes, l'institut du thorax, Service de Cardiologie, Nantes, France. [8]CHU Rouen, Département de Cardiologie, Rouen, France. [9]Department of Cardiology, Thoraxcenter, University Medical Center Groningen, Groningen, The Netherlands. [10]Institut für Humangenetik, Technical University of Munich, Munich, Germany. [11]Helmholtz Zentrum Munich, German Research Center for Environmental Health, Neuherberg, Germany. [12]Department of Medicine I, Ludwig-Maximilians-University Munich, Klinikum Großhadern, Munich, Germany. [13]Department of Cardiology, Ege University School of Medicine, Izmir, Turkey.

Brugada syndrome is a genetic disease associated with sudden cardiac death that is characterized by ventricular fibrillation and right precordial ST segment elevation on ECG. Loss-of-function mutations in *SCN5A*, which encodes the predominant cardiac sodium channel α subunit $Na_V1.5$, can cause Brugada syndrome and cardiac conduction disease. However, *SCN5A* mutations are not detected in the majority of patients with these syndromes, suggesting that other genes can cause or modify presentation of these disorders. Here, we investigated *SCN1B*, which encodes the function-modifying sodium channel β1 subunit, in 282 probands with Brugada syndrome and in 44 patients with conduction disease, none of whom had *SCN5A* mutations. We identified 3 mutations segregating with arrhythmia in 3 kindreds. Two of these mutations were located in a newly described alternately processed transcript, β1B. Both the canonical and alternately processed transcripts were expressed in the human heart and were expressed to a greater degree in Purkinje fibers than in heart muscle, consistent with the clinical presentation of conduction disease. Sodium current was lower when $Na_V1.5$ was coexpressed with mutant β1 or β1B subunits than when it was coexpressed with WT subunits. These findings implicate *SCN1B* as a disease gene for human arrhythmia susceptibility.

Introduction

Voltage-gated sodium channels are critical for the generation and propagation of the cardiac action potential, and mutations in *SCN5A*, the gene encoding the major pore-forming sodium channel α subunit in the heart ($Na_V1.5$), cause multiple cardiac arrhythmia syndromes (1–4). Mutations producing enhanced inward current during the course of the action potential plateau, often as a consequence of destabilized fast inactivation of the channel, cause long QT syndrome type 3 (LQT3; OMIM 603830) (1). On the other hand, a reduction in sodium current leads to cardiac conduction disease, which may be progressive (OMIM 113900) (2, 3), and Brugada syndrome (OMIM 601144), characterized by ST segment elevation in the right precordial leads (V1 to V3) of the 12-lead ECG and episodes of ventricular fibrillation (4). Multiple mechanisms have been described that reduce sodium current in these syndromes, including altered gating of the channel or reduced cell-surface expression (5). In addition, mutations in *SCN5A* may manifest with an overlap of these different phenotypes (6–10). However, mutations in *SCN5A* are found in fewer than 30% of patients with Brugada syndrome, indicating involvement of other genes (11). A mutation in the glycerol-3-phosphate dehydrogenase 1–like gene (*GPD1L*) has recently been reported in a large kindred with Brugada syndrome (12); however, *GPD1L* mutations are rare in Brugada syndrome (13). Antzelevitch et al. have recently reported mutations in the gene encoding the L-type calcium channel (*CACNA1C*) or its β2b subunit (*CACNB2b*) in Brugada syndrome patients with unusually short QT intervals (14), but the frequency of these defects as a cause for more-typical Brugada syndrome is unknown. *SCN5A* mutations are also not identified in the majority of patients with cardiac conduction disease (15).

Sodium channels are multisubunit protein complexes composed not only of pore-forming α subunits but also of multiple other protein partners including auxiliary function-modifying β subunits (16, 17). In humans, 4 sodium channel β subunits (β1 to β4, encoded by *SCN1B* to *SCN4B*) have been identified, and they share a common predicted protein topology: a large extracellular N-terminal domain (including an immunoglobulin-like domain), a single transmembrane segment, and an intracellular C-terminal domain (16). Functions attributed to β subunits include an increase in sodium channel expression at the cell surface, modulation of channel gating and voltage dependence, and a role in cell adhesion and recruitment of cytosolic proteins such as ankyrin-G (16).

The β1 transcript arises from splicing of exons 1–5 of the *SCN1B* gene (Figure 1, A and B). More recently, a second transcript has been described, arising from splicing of exons 1–3 with retention of a segment of intron 3 (termed exon 3A), leading to an alternate 3′ sequence

Conflict of interest: The authors have declared that no conflict of interest exists.
Citation for this article: *J. Clin. Invest.* **118**:2260–2268 (2008). doi:10.1172/JCI33891.

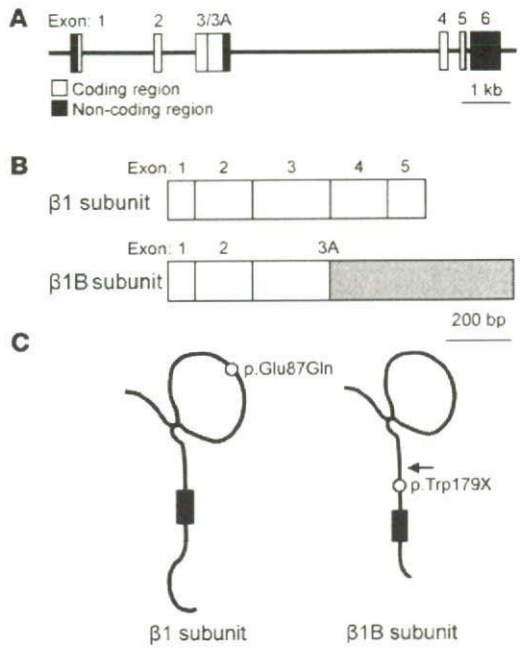

Figure 1
Structure of β1 and β1B subunits. (**A**) Genomic structure of *SCN1B*. (**B**) Extension of exon 3 (c.208–458) into intron 3 creates a novel 3′ end of the transcript (exon 3A, c.208–978) and generates an alternate transcript encoding β1B. The gray region indicates the unique sequence of exon 3A. (**C**) Predicted topology of β1 and β1B. The β1B protein has unique juxtamembrane, transmembrane, and intracellular domains. The arrow indicates the initial amino acid of the β1B-specific segment. Circles indicate the locations of the mutations.

(Figure 1, A and B) (18, 19). This latter transcript encodes the β1B subunit, which, in spite of the different 3′ sequence, has a predicted protein topology similar to that of β1 (Figure 1C) (19). The β1B subunit has been shown to increase a neuronal sodium current ($Na_v1.2$) (19), but its effects on $Na_v1.5$ current have not yet been investigated, although β1 and β1B are both expressed in heart (19, 20).

Since loss-of-function $Na_v1.5$ mutations cause conduction disease and Brugada syndrome, one could envision that mutations in sodium channel β subunits could also underlie these disorders by decreasing sodium current. Therefore, we tested the hypothesis that mutations in *SCN1B* coding sequences, for either β1 or β1B, underlie cases of conduction disease and Brugada syndrome. We identified 3 mutations segregating with arrhythmia in 3 kindreds, and 2 of the mutations were located in the newly described β1B transcript. Both β1 and β1B transcripts were expressed in the human heart and were abundant in Purkinje fibers that play a critical role in electric pulse conduction in heart. Electrophysiologic study of heterologously expressed sodium channels revealed loss of sodium current with mutant subunits.

Results

Mutation analysis and clinical data. We screened 282 probands with Brugada syndrome and 44 with conduction disease for mutations in exons 1–5 of *SCN1B* encoding the β1 subunit and in exon 3A retained in the β1B transcript (Figure 1, A and B). *SCN5A* coding region mutations had been previously excluded in all 326 subjects. Three variants were identified in probands and family members (Figure 2A). These variants were absent in 1,404 population controls (see Methods).

A missense mutation, c.259G→C (Figure 2B) in exon 3, resulting in p.Glu87Gln within the extracellular immunoglobulin loop of the protein (Figure 1C) was identified in a Turkish kindred affected by conduction disease (family 1; Figure 2A). Alignment of the β1 subunit amino acid sequence from multiple species demonstrated that Glu87 is highly conserved, supporting the importance of glutamate at this position (Figure 2C). The proband was a 50-year-old white Turkish female (II-1) who presented with palpitations and dizziness. Physical examination and echocardiography were normal, and her ECG showed complete left bundle branch block. A clinical electrophysiological study revealed a prolonged His-ventricle interval of 80 ms and inducible atrioventricular nodal reentrant tachycardia; complete atrioventricular block occurred following atrial programmed stimulation and during induced tachycardia. A dual-chamber pacemaker was implanted with resolution of symptoms. The same mutation was found in her brother (II-3), who had bifascicular block (right bundle branch block and left anterior hemiblock), and her mother (I-2), who had a normal ECG. There was no family history of syncope, sudden cardiac death, or epilepsy.

A nonsense mutation, c.536G→A in exon 3A (Figure 1B and Figure 2D), was identified in a French kindred affected with Brugada syndrome and conduction disease (family 2; Figure 2A). This mutation results in p.Trp179X and is predicted to generate a prematurely truncated protein lacking the membrane-spanning segment and intracellular portion of the protein (Figure 1C). The proband was a 53-year-old white male (II-4) who presented with chest pain. Physical examination, echocardiography, and coronary angiography were normal. His ECG showed ST segment elevation typical of Brugada syndrome and conduction abnormalities (prolonged PR interval of 220 ms and left anterior hemiblock; Figure 2E) (21). Ventricular fibrillation was induced by programmed electrical stimulation in basal state (in the absence of drugs). The same mutation was detected in his brother (II-1), nephew (III-1), and sister (II-2). The brother had no palpitations or history of syncope. His baseline ECG showed left anterior hemiblock and minor ST segment elevation suggestive of Brugada syndrome at baseline (type II saddleback abnormality; ref. 21); with flecainide challenge, the ST segment elevation was further exaggerated but did not meet criteria for a diagnostic (type I) pattern. The nephew had right bundle branch block and type II Brugada syndrome ECG after flecainide challenge, and the sister had a normal ECG and a negative flecainide test. There was no family history of tachyarrhythmias, syncope, sudden cardiac death, or epilepsy.

A different nonsense mutation, c.537G→A in exon 3A (Figure 2D), resulting in p.Trp179X, affecting the same codon as in family 2, was identified in a Dutch kindred (family 3; Figure 2A). The proband was a 17-year-old white female (II-1). Physical examination and echocardiography were normal, and a flecainide test for Brugada syndrome was negative. Her ECG showed right bundle branch block and prolonged PR interval of 196 ms (normal upper limit in teenagers, 180 ms) (22). The same mutation was found in her father (I-1), with normal ECG and negative flecainide test. The family history was negative for syncope, sudden cardiac death, or epilepsy.

β1 and β1B transcript expression. To confirm and extend previous reports that β1B is expressed in brain, heart, skeletal muscle, and other organs (19), we used quantitative real-time PCR in nondiseased